



Missouri University of Science and Technology  
Scholars' Mine

---

Center for Cold-Formed Steel Structures Library

Wei-Wen Yu Center for Cold-Formed Steel Structures

---

01 May 1995

## The effect of flange restraint on web crippling strength of cold-formed steel Z- and I-sections

Darryl E. Cain

Roger A. LaBoube

*Missouri University of Science and Technology*, [laboube@mst.edu](mailto:laboube@mst.edu)

Wei-wen Yu

*Missouri University of Science and Technology*, [wwy4@mst.edu](mailto:wwy4@mst.edu)

Follow this and additional works at: <https://scholarsmine.mst.edu/ccfss-library>

 Part of the [Structural Engineering Commons](#)

---

### Recommended Citation

Cain, Darryl E.; LaBoube, Roger A.; and Yu, Wei-wen, "The effect of flange restraint on web crippling strength of cold-formed steel Z- and I-sections" (1995). *Center for Cold-Formed Steel Structures Library*. 105.

<https://scholarsmine.mst.edu/ccfss-library/105>

This Technical Report is brought to you for free and open access by Scholars' Mine. It has been accepted for inclusion in Center for Cold-Formed Steel Structures Library by an authorized administrator of Scholars' Mine. This work is protected by U. S. Copyright Law. Unauthorized use including reproduction for redistribution requires the permission of the copyright holder. For more information, please contact [scholarsmine@mst.edu](mailto:scholarsmine@mst.edu).

**Civil Engineering Study 95-2  
Cold-Formed Steel Series**

**Final Report**

**THE EFFECT OF FLANGE RESTRAINT ON WEB CRIPPLING STRENGTH  
OF COLD-FORMED STEEL Z- AND I- SECTIONS**

by

**Darryl E. Cain  
Research Assistant**

**Roger A. LaBoube  
Wei-Wen Yu  
Project Directors**

**A Research Project Sponsored by  
the American Iron and Steel Institute  
and  
Metal Building Manufacturers Association**

**May 1995**

**Department of Civil Engineering  
Center for Cold-Formed Steel Structures  
University of Missouri-Rolla  
Rolla, Missouri**

## PREFACE

When considering the web crippling strength of a cold-formed steel member, the current edition of the AISI Specification for the Design of Cold-Formed Steel Structural Members does not distinguish between the behavior of a member having its flanges attached to a support member, and a member not attached to its support. To enhance the industry and design professional's understanding of web crippling, a study was initiated at the University of Missouri-Rolla to explore the influence of flange attachment.

This research consisted of web crippling tests on identical specimens. The specimens were tested where either cross sections were attached to a support beam or were not attached to the support beam. This enabled direct comparison and evaluation of flange attachment. The results were compared with AISI design criteria and other prediction equations, and suggested design recommendations were developed.

This report is based on the thesis presented to the Faculty of the Graduate School of the University of Missouri-Rolla in partial fulfillment of the requirements for the degree of Masters of Science in Civil Engineering.

This investigation was sponsored by the American Iron and Steel Institute and the Metal Building Manufacturers Association. The technical guidance provided by the AISI Subcommittee on Flexural Members and the AISI Staff is gratefully acknowledged. Members of the AISI Subcommittee are: J. N. Nunnery (chairman), R. E. Albrecht, R. E. Brown, C. R. Clauer, D. S. Ellifritt, S. J. Errera, J. M. Fisher, T. V. Galambos, M. Golovin, G. J. Hancock, A. J. Harold, R. B. Heagler, D. L. Johnson, W. J. Kile, R. A. LaBoube, M. R. Loeske, R. Madsen, T. M. Murray, T. B. Pekoz, R. M. Schuster, P. A. Seaburg, T. Sputo, T. W. Trestain, and

W. W. Yu. The AISI Staff include R. B. Haws and K. L. Slaughter. Thanks are also extended to W. L. Shoemaker of the Metal Building Manufacturers Association for his assistance.

## TABLE OF CONTENTS

	Page
PREFACE .....	iii
LIST OF ILLUSTRATIONS .....	vii
LIST OF TABLES .....	ix
 SECTION	
I. INTRODUCTION .....	1
A. GENERAL .....	1
B. PURPOSE OF INVESTIGATION .....	3
C. SCOPE OF INVESTIGATION .....	3
II. REVIEW OF LITERATURE .....	5
A. GENERAL .....	5
B. ANALYTICAL STUDY .....	5
1. Opposite Uniformly Distributed Loads .....	6
2. Opposite Concentrated Loads .....	8
3. Opposite Locally Distributed Edge Loads .....	8
4. Locally Distributed Edge Load .....	11
5. Member Behavior .....	11
C. EXPERIMENTAL STUDY .....	14
D. CURRENT DESIGN APPROACHES .....	17
1. AISI Specification .....	17

## TABLE OF CONTENTS (Cont'd.)

	Page
2. Prabakaran and Schuster Equations . . . . .	18
3. Santaputra, Parks, and Yu Equations . . . . .	23
III. EXPERIMENTAL INVESTIGATION . . . . .	29
A. GENERAL . . . . .	29
B. TEST SPECIMENS . . . . .	31
C. TEST PROCEDURES . . . . .	42
1. Z-Sections . . . . .	42
2. I-Sections . . . . .	46
IV. TEST RESULTS AND EVALUATION OF DATA . . . . .	54
A. GENERAL . . . . .	54
B. TEST RESULTS . . . . .	54
1. Z-Sections . . . . .	54
2. I-Sections . . . . .	73
C. EVALUATION OF RESULTS . . . . .	83
1. Statistical Comparison of Results . . . . .	83
2. Z-Sections . . . . .	85
3. I-Sections . . . . .	86
D. DEVELOPMENT OF FLANGE RESTRAINT FACTOR FOR Z-SECTIONS . . . . .	87
V. PROPOSED DESIGN RECOMMENDATIONS . . . . .	91
VI. CONCLUSIONS . . . . .	92
BIBLIOGRAPHY . . . . .	93

## LIST OF ILLUSTRATIONS

Figure	Page
1 Rectangular Plate Subjected to Uniformly Distributed Loads [18, 20] . . . . .	7
2 Rectangular Plate Subjected to Opposite Concentrated Loads [10, 13, 20] . . . . .	9
3 Rectangular Plate Subjected to Opposite Locally Distributed Edge Loads [16, 20] . . . . .	10
4 Rectangular Plate Subjected to a Locally Distributed Edge Force [14, 20] . . . . .	12
5 Plate Buckling Coefficients, k, for Eq. 2.7 [17, 20] . . . . .	13
6 Web Crippling Loading Conditions [4, 7] . . . . .	16
7 Application of Design Equations Listed in Table I [3] . . . . .	22
8 Santaputra, Parks and Yu Web Crippling Equation Parameter Definitions for EOF Loading Condition . . . . .	26
9 Santaputra, Parks and Yu Web Crippling Equation Parameter Definitions for IOF Loading Condition . . . . .	26
10 Tinius Olson Universal Testing Machine . . . . .	30
11 Cross Section View of a Z-Section Specimen [6] . . . . .	33
12 Cross Section View of an I-Section Specimen [6] . . . . .	33
13 Typical Bearing Conditions for EOF and IOF Loading Conditions [6] . . . . .	40
14 EOF and IOF Loading Condition Stiffener Locations [6] . . . . .	41
15 Photograph of Typical Failure of a Z-Section with Cross-Bracing Subjected to EOF Loading Condition with Unrestrained Flanges . . . . .	47

## LIST OF ILLUSTRATION (Cont'd.)

Figure	Page
16 Photograph of Typical Failure of a Z-Section with Cross-Bracing Subjected to EOF Loading Condition with Restrained Flanges . . . . .	47
17 Photograph of a Typical Failure of Z-Section Subjected to EOF Loading Condition with Unrestrained Flanges . . . . .	48
18 Photograph of a Typical Failure of Z-Section Subjected to EOF Loading Condition with Restrained Flanges . . . . .	48
19 Typical Bolt Patterns for I-Beams . . . . .	50
20 Top View of Typical Connection of an I-Beam with Flanges Restrained [6] . . . . .	51
21 Photograph of Typical I-Beam Subjected to IOF Loading Condition with Restrained Flanges with Bolt Pattern One . . . . .	52
22 Photograph of a Typical I-Beam Subjected to IOF Loading Condition with Restrained Flanges with Bolt Pattern Two . . . . .	52
23 Photograph of a Typical I-Beam Subjected to IOF Loading Condition with Restrained Flanges with Bolt Pattern Three . . . . .	53
24 Graph of $P_f/P_{wf}$ vs. $h/t$ for Fastened Flange Z-Sections Showing the Suggested Modification Curve . . . . .	89
25 Graph of $P_f/P_{wf}$ vs. $h/t$ for Fastened Flange Z-Sections Including Bhakta Data Points . . . . .	90



## LIST OF TABLES

Table	Page
I ALLOWABLE STRENGTH ( $P_u$ ) . . . . .	19
II RECOMMENDED EXPRESSION . . . . .	24
III TEST PROGRAM . . . . .	31
IV MATERIAL PROPERTIES AND THICKNESSES OF SECTIONS USED IN THE EXPERIMENTAL STUDIES . . . . .	32
V MEASURED DIMENSIONS OF Z-SECTIONS . . . . .	34
VI MEASURED DIMENSIONS OF I-SECTIONS . . . . .	38
VII EQUATION PARAMETERS AND TEST DATA OF Z-SECTIONS . . . . .	43
VIII EQUATION PARAMETERS AND TEST DATA OF I-SECTIONS . . . . .	45
IX SUMMARY OF ALL Z-SECTION PARAMETERS, TEST LOADS, AND AISI COMPUTED LOADS . . . . .	56
X SUMMARY OF ALL Z-SECTION PARAMETERS, TEST LOADS, AND PRABAKARAN COMPUTED LOADS . . . . .	57
XI SUMMARY OF ALL Z-SECTION PARAMETERS, TEST LOADS, AND SANTAPUTRA COMPUTED LOADS . . . . .	58
XII SUMMARY OF ALL Z-SECTION PARAMETERS, TEST LOADS, AND AISI COMPUTED LOADS . . . . .	59
XIII SUMMARY OF ALL Z-SECTION PARAMETERS, TEST LOADS, AND PRABAKARAN COMPUTED LOADS . . . . .	60
XIV SUMMARY OF ALL Z-SECTION PARAMETERS, TEST LOADS, AND SANTAPUTRA COMPUTED LOADS . . . . .	61
XV SUMMARY OF ALL Z-SECTION PARAMETERS, TEST LOADS, AND AISI COMPUTED LOADS . . . . .	62

## LIST OF TABLES (Cont'd.)

Table	Page
XVI SUMMARY OF ALL Z-SECTION PARAMETERS, TEST LOADS, AND PRABAKARAN COMPUTED LOADS . . . . .	63
XVII SUMMARY OF ALL Z-SECTION PARAMETERS, TEST LOADS, AND SANTAPUTRA COMPUTED LOADS . . . . .	64
XVIII SUMMARY OF ALL Z-SECTION PARAMETERS, TEST LOADS, AND AISI COMPUTED LOADS . . . . .	65
XIX SUMMARY OF ALL Z-SECTION PARAMETERS, TEST LOADS, AND PRABAKARAN COMPUTED LOADS . . . . .	66
XX SUMMARY OF ALL Z-SECTION PARAMETERS, TEST LOADS, AND SANTAPUTRA COMPUTED LOADS . . . . .	67
XXI SUMMARY OF ALL I-SECTION PARAMETERS, TEST LOADS, AND AISI MULTIPLE WEB EQUATION COMPUTED LOADS . . . . .	74
XXII SUMMARY OF ALL I-SECTION PARAMETERS, TEST LOADS, AND AISI SINGLE WEB EQUATION COMPUTED LOADS . . . . .	75
XXIII SUMMARY OF ALL I-SECTION PARAMETERS, TEST LOADS, AND PRABAKARAN COMPUTED LOADS . . . . .	76
XXIV SUMMARY OF ALL I-SECTION PARAMETERS, TEST LOADS, AND SANTAPUTRA COMPUTED LOADS . . . . .	77
XXV SUMMARY OF ALL I-SECTION PARAMETERS, TEST LOADS, AND AISI MULTIPLE WEB EQUATION COMPUTED LOADS . . . . .	78
XXVI SUMMARY OF ALL I-SECTION PARAMETERS, TEST LOADS, AND AISI SINGLE WEB EQUATION COMPUTED LOADS . . . . .	79
XXVII SUMMARY OF ALL I-SECTION PARAMETERS, TEST LOADS, AND PRABAKARAN COMPUTED LOADS . . . . .	80

## LIST OF TABLES (Cont'd.)

Table	Page
XXVIII SUMMARY OF ALL I-SECTION PARAMETERS, TEST LOADS, AND SANTAPUTRA COMPUTED LOADS . . . . .	81
XXIX STATISTICAL DATA . . . . .	84

## I. INTRODUCTION

### A. GENERAL

In today's steel construction there are two main types of structural steel members. The most familiar type is the hot-rolled steel member, and the less familiar type is the cold-formed steel member. Cold-formed steel may be the lesser known of the two types of structural steel members available to structural designers, however, cold-formed steel members are increasingly becoming the steel member of choice by many structural designers in today's competitive construction market. Cold-formed steel members are used today in many areas of design such as building construction, automotive bodies, bridge construction, storage racks, and highway products. Cold-formed simply means that a piece of flat rolled steel is processed to final form by shaping it at ambient temperature [1]. The three methods that are generally used in the manufacture of cold-formed sections are roll-forming, press-brake forming, and bending-brake forming [2].

Many analytical and experimental studies have been performed in an attempt to accurately predict the strength and behavior of cold-formed steel structural members. The web crippling strength of cold-formed steel sections can be calculated by using the appropriate equations found in the "Specification for the Design of Cold-Formed Steel Structural Members (1989 Addendum)" [3] of the American Iron and Steel Institute, hence referred to as AISI Specification. The specification equations for web crippling strength are primarily based on experimental data compiled by Winter and Pian [4] at Cornell University and Hetrakul and Yu [5] at the University of Missouri-Rolla. These researchers have developed design equations that enable the design engineer to estimate

the following web crippling limit states; end one-flange loading (EOF), interior one-flange loading (IOF), end two-flange loading (ETF), and interior two-flange loading (ITF).

A cold-formed steel section may be loaded by inducing a concentrated load into the web at either the load application point between supports or by way of the reaction at the support. The specification equations, for some cases, may not reflect the actual field practices because the equations developed, for the above mentioned limit states, were primarily based on test results in which the flange was not attached to the support beam. This support condition may not represent accurate field practices used in some situations. In some cases, the flanges of sections are not fastened to the support members, and the existing AISI Specification equations estimate the web crippling strength accurately. But, in other cases, the flanges are either bolted or welded to the support members. Due to the restraining affect of the fasteners, the AISI Specification equations may underestimate the web crippling strength of the member.

In 1992 Bhakta et al. [6] conducted a pilot study that focused on the influence of flange restraint on the web crippling capacity of industry standard C- and Z- sections. The study's results identified both conservatism and unconservatism in the application of the AISI Specification web crippling provisions. To further explore the conservative web crippling behavior of flange restrained Z-sections subjected to an EOF loading condition and the unconservative web crippling behavior of I-sections subjected to IOF loading condition, further study was initiated at the University of Missouri-Rolla in 1994. Based on the findings of this study, and the previous work of Bhakta, design recommendations were developed and presented herein.

## B. PURPOSE OF INVESTIGATION

The purpose of this experimental and analytical study was to explore the web crippling behavior of Z- and I-sections which are being used in building construction. This study focused only on the end one-flange loading (EOF) condition of Z-sections to further study the web crippling capacity of the Z-section members with their flanges fastened to the support. This study also focused only on the interior one-flange loading (IOF) condition of back-to-back C-sections that form I-sections. The IOF study addressed the effect of different bolt configurations used to inter-connect the C-sections. The IOF loading condition of Z-sections and the EOF loading condition of I-sections were not investigated due to the recommendations and findings of the pilot study performed by Bhakta in 1992. The research findings were used to develop suggested design modifications for web crippling strength of fastened flange Z-sections subjected to an EOF loading condition.

## C. SCOPE OF INVESTIGATION

This study consisted primarily of experimental investigations of cold-formed steel Z- and I-section members with flanges affixed to supports and members with flanges not fixed to supports. The study was restricted to the investigation of these cold-formed steel sections subjected to web crippling alone. The test members considered in this investigation are edge-stiffened cold-formed steel Z- and I-sections.

The first step of this investigation was to research and study available reports and technical publications relative to the behavior of cold-formed steel members subjected to web crippling failure. A summary of previous research reports, technical publications,

and theses related to the web crippling strength of cold-formed steel sections is contained in Section II, Review of Literature.

The experimental study of beam webs subjected to web crippling only is discussed in Section III, Experimental Investigation. Details of test specimens and test procedures are also discussed in this section.

In Section IV, Test Results and Evaluation of Data, the results of tests conducted in this phase of investigation are evaluated by comparing the tested failure loads to the predicted ultimate web crippling loads calculated by three methods, 1) the present AISI Specification's design equations, 2) the Prabakaran and Schuster [7] equations, and 3) the Santaputra, Parks, and Yu [8] equations. Note that for all three methods used in this comparison, that each equation was developed by using web crippling strength data without the restraint of flanges. Therefore, it is expected that these methods stated above may underestimate the fastened flange tested failures results. Both Z- and I-sections tested are discussed in this section. This section also discusses the comparison of the test results with beam flanges fastened to supports, to the results of the tests with beam flanges not fastened to supports. The research findings were used to develop suggested design modifications for web crippling strength of fastened flange Z-sections subjected to an EOF loading condition.

Section V, Proposed Design Recommendations, presents the recommendations of this study for the best existing design criteria to use for determining the web crippling strength of cold-formed steel Z- and I-section members. Finally, Section VI, Conclusions, presents the conclusions found in this investigation.

## II. REVIEW OF LITERATURE

### A. GENERAL

In the initial stage of this investigation, several publications and research reports were carefully studied. They related to previous analytical and experimental studies of the strength of web plates subjected to web crippling and a combination of web crippling and bending moment. The combination of web crippling and bending moment is not discussed because the study concentrated on webs subjected to web crippling only. In Section II.B a brief history of some theoretical approaches is reviewed. Section II.C contains a historic review of the key experimental approaches. And in Section II.D the present available design criteria for preventing web crippling are reviewed.

### B. ANALYTICAL STUDY

The theoretical background for the problem of web crippling has been studied. The flange and web of cold-formed steel sections are interactive, but it is ideal to consider the behavior of webs of cold-formed steel sections as rectangular flat plates with simple supports along the edges which are subjected to locally distributed in-plane edge forces. Thin, flat plates are associated with problems primarily due to instability. A brief overview of elastic plate buckling is presented. Elastic plate buckling problems of simply supported thin, flat plates are the simplest to analyze and have given rise to a substantial amount of published literature. However, some stiffened compression elements will not collapse when the elastic buckling load is reached, but will develop postbuckling strength by means of redistribution of stress. The buckling of separate flat,



rectangular plates under locally distributed edge forces has been studied by numerous investigators [2], including Sommerfeld [9], Timoshenko [10], Leggett [11], Hopkins [12], Yamaki [13], Zetlin [14], White and Cottingham [15], Khan and Walker [16], Khan, Johns, and Hayman [17], and others. These studies are summarized into four different edge loading categories which are as follows:

1. Opposite Uniformly Distributed Loads: By solving Bryan's differential equation based on small deflection theory, the critical buckling stress of a simply supported plate subjected to two opposite uniformly distributed loads as shown in Figure 1a can be determined as follows:

$$\frac{\partial^4 \omega}{\partial x^4} + 2 \frac{\partial^4 \omega}{\partial x^2 \partial y^2} + \frac{\partial^4 \omega}{\partial y^4} + \frac{f_x t}{D} \frac{\partial^2 \omega}{\partial x^2} = 0 \quad (\text{Eq. 1})$$

where

$$D = \frac{Et^3}{12(1-\mu^2)} \quad (\text{Eq. 2})$$

and  $E$  = modulus of elasticity of cold-formed steel = 29,500 ksi

$t$  = thickness of plate

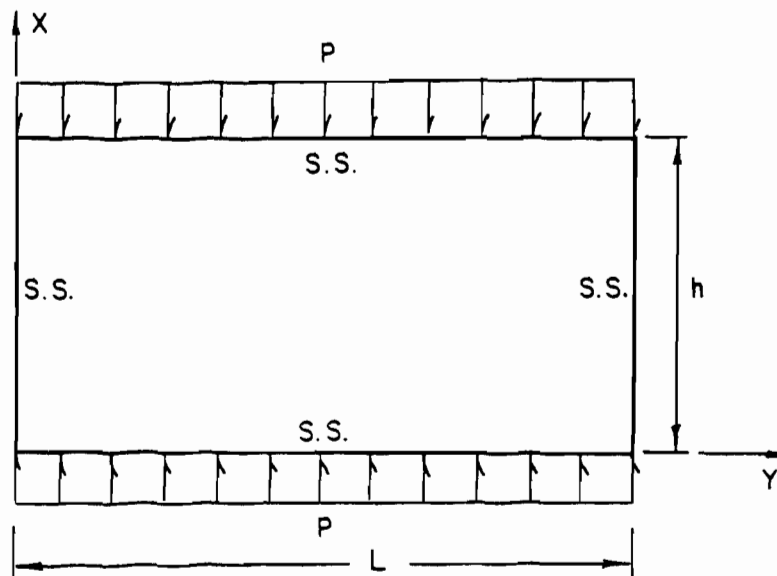
$\mu$  = Poisson's ratio = 0.3 for steel in the elastic range

$\omega$  = deflection of plate perpendicular to surface

$f_x$  = compression stress in x direction

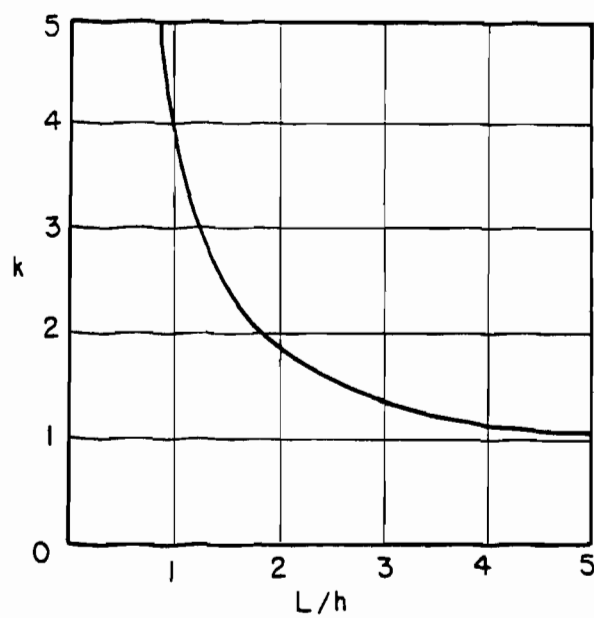
The solution of Eq. 1 is explained by Yu [2]. The obtained solution is an equation for the critical elastic buckling load [10]:

$$P_{cr} = \frac{k\pi^2 DL}{h^2} \quad (\text{Eq. 3})$$



S.S. = simply supported

(a) Plate Loading



(b) Plate Buckling Coefficient,  $k$

Figure 1. Rectangular Plate Subjected to Uniformly Distributed Loads [<sup>18, 20</sup>]

where  $P_{cr}$  = elastic critical buckling load  
 $k$  = buckling coefficient  
 $L$  = span length, in.  
 $h$  = clear distance between flanges measured along the plane of web, in.

The values of buckling coefficient,  $k$ , are shown in Figure 1b. Note that for a square plate,  $L/h = 1$ , the value of  $k$  equals 4.

2. Opposite Concentrated Loads: Timoshenko [10] and other researchers [13] derived Eq. 4 to compute the elastic critical buckling load of a simply supported rectangular plate subjected to equal and opposite concentrated forces as shown in Figure 2a:

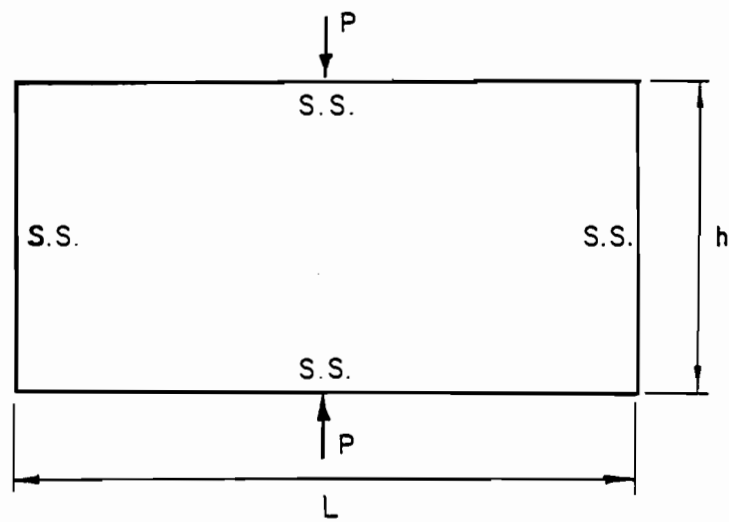
$$P_{cr} = \frac{k\pi D}{h} \quad (\text{Eq. 4})$$

Yamaki [13] studied the buckling of a rectangular plate subjected to equal and opposite concentrated forces on the edges with different boundary conditions and summarized the variation of  $k$  with  $L/h$  as shown in Figure 2b.

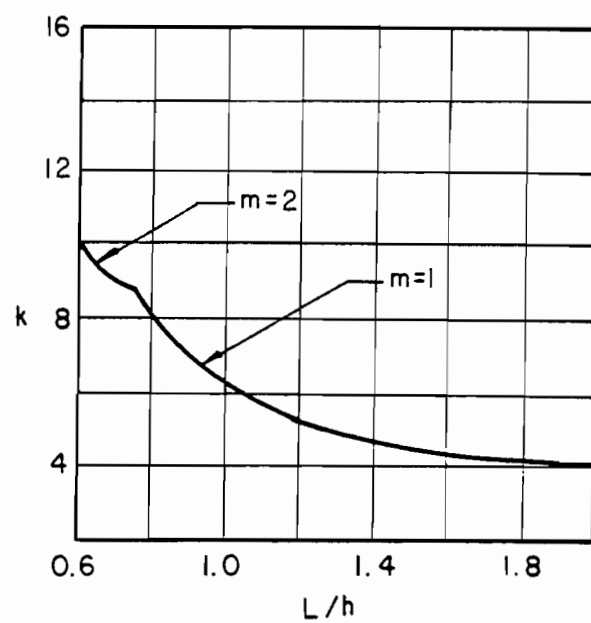
3. Opposite Locally Distributed Edge Loads: For plates subjected to locally distributed edge forces as shown in Figure 3a, Khan and Walker [16] developed the following elastic critical buckling load:

$$P_{cr} = \frac{k\pi^2 D}{h} \quad (\text{Eq. 5})$$

Figure 3b gives the values of the buckling coefficient,  $k$ , as the function of  $L/h$  ratio for two different ratios of  $N/h$ .

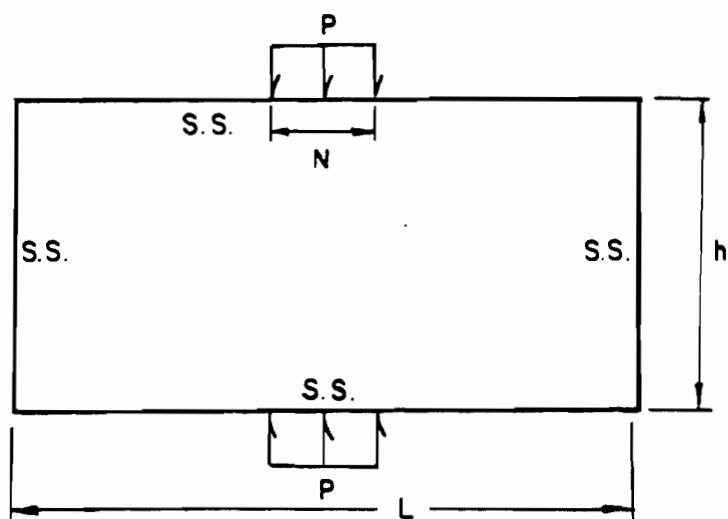


(a) Plate Loading



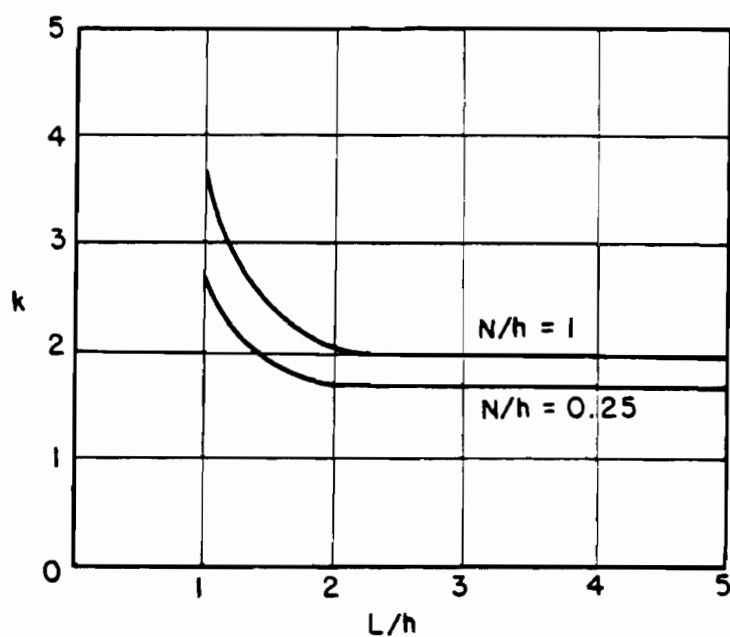
(b) Plate Buckling Coefficient, k

Figure 2. Rectangular Plate Subjected to Opposite Concentrated Loads [10, 13, 20]



$N$  = bearing length of load

(a) Plate Loading



(b) Plate Buckling Coefficient,  $k$

Figure 3. Rectangular Plate Subjected to Opposite Locally Distributed Edge Loads [16, 20]

4. Locally Distributed Edge Load: Zetlin [14] studied the problem of buckling of a simply supported plate subjected to a locally distributed edge load applied symmetrically about the mid-span section, and derived the following critical buckling load equation:

$$P_{cr} = \frac{k\pi^2 D}{L} \quad (\text{Eq. 6})$$

Figure 4a shows Zetlin's loading configuration. The values that Zetlin obtained for the buckling coefficient,  $k$ , are shown graphically in Figure 4b.

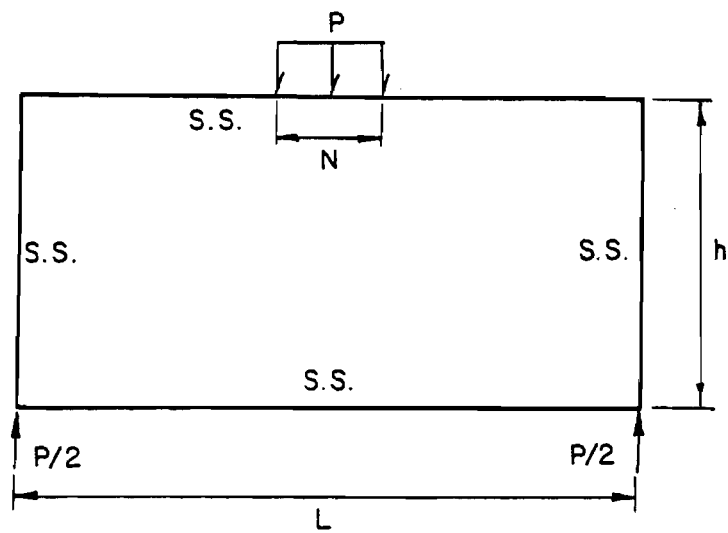
Another study for buckling of a simply supported plate subjected to a locally distributed edge load was conducted by Khan, Johns and Hayman [17]. These researchers used the same loading configuration as Zetlin (Figure 4a) and derived the following critical buckling load equation:

$$P_{cr} = \frac{k\pi^2 D}{h} \quad (\text{Eq. 7})$$

Figure 5 contains the graphical results of the buckling coefficients,  $k$ , derived by Khan, Johns and Hayman to be used with Eq. 7.

5. Member Behavior: The theoretical analysis of web crippling for cold-formed steel flexural members is extremely complicated for beams having webs connected to flanges because it involves the following factors: [2]

1. Nonuniform stress distribution under the applied load.
2. Elastic and inelastic stability of the web element.
3. Local yielding in the immediate region of the load application.



(a) Plate Loading

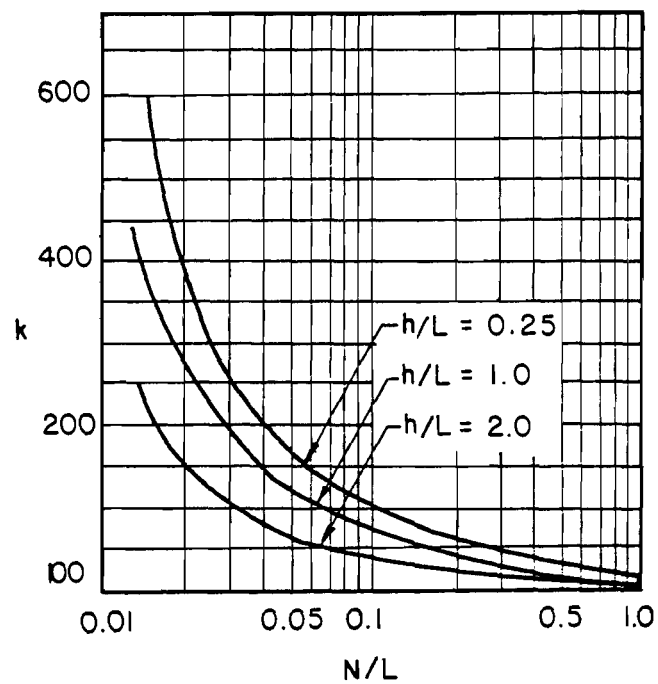
(b) Plate Buckling Coefficient,  $k$ 

Figure 4. Rectangular Plate Subjected to a Locally Distributed Edge Load [14, 20]

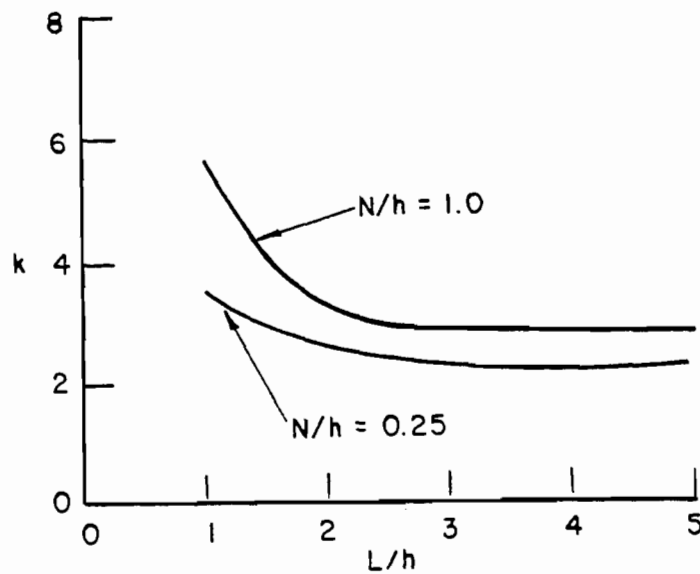


Figure 5. Plate Buckling Coefficients,  $k$ , for Eq. 2.7 [17, 20]

4. Bending produced by eccentric load when it is applied on the bearing flange at a distance beyond the curved transition of the web.
5. Initial out-of-plane imperfection of plate elements.
6. Various edge restraints provided by beam flanges and the interaction between flange and web elements.

A recent analytical investigation concerning the web crippling behavior of thin-walled members subjected to the combined forces of a concentrated load and a bending moment was conducted by Bakker, Peköz and Stark [19]. This study was based on yield line analysis of failure mechanisms and found that the corner radius largely affected the type of mechanism formed [6].



As stated by Santaputra and Yu [20], "Mathematical difficulties arising from the nature of complex stress field associated with this problem prohibit an exact solution." Santaputra and Yu [20] provide a summary of the researchers who have attempted to use the finite element and finite strip methods to predict the ultimate web crippling load. The previous investigations discussed by Santaputra and Yu [20] are based on Bagchi and Rockey [21], Rockey and Bagchi [22], Rockey, El-gaaly, and Bagchi [23], Graves Smith and Sridharan [24], Gierlinski and Graves Smith [25], and Lee, Harris, and Hsu [26]. Due to the difficulties associated with the theoretical analysis, most desired web crippling design expressions have been developed experimentally.

### C. EXPERIMENTAL STUDY

As stated in Section II.B, stiffened compression elements will not collapse when the elastic buckling load is reached, but will develop sizable postbuckling strength. However, Walker [1] states that developing an equation to compute the postbuckling strength is not an easy task. This is primarily due to the complex nature of the numerous parameters affecting the web crippling strength and the mathematical difficulties encountered in the analysis.

The present AISI design provisions for web crippling are based on the extensive experimental investigations conducted by Winter and Pian [4], and Zetlin [14] and more recently at the University of Missouri-Rolla by Hetrakul and Yu [5]. These experimental investigations studied the following four loading conditions for beams having single unreinforced webs and for I-beams [2]:

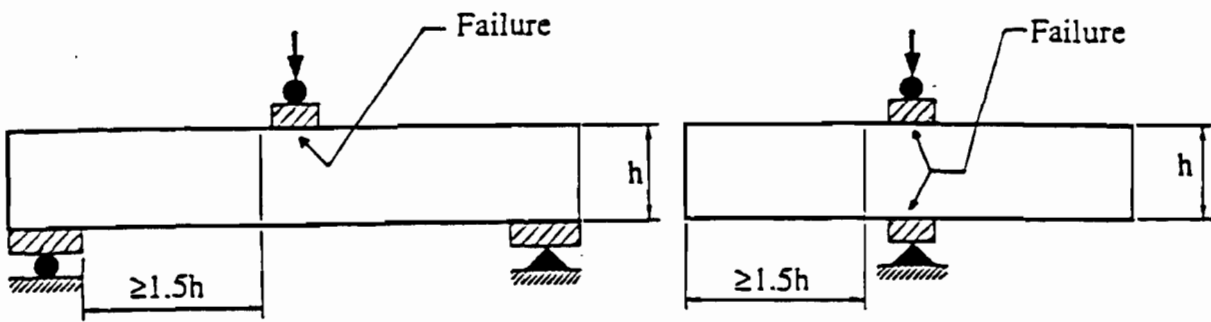
1. End one-flange loading (EOF)

2. Interior one-flange loading (IOF)
3. End two-flange loading (ETF)
4. Interior two-flange loading (ITF)

These loading conditions are shown in Figure 6. The distance of no less than 1.5 times the web depth between bearing plates is to avoid the effect of two-flange action.

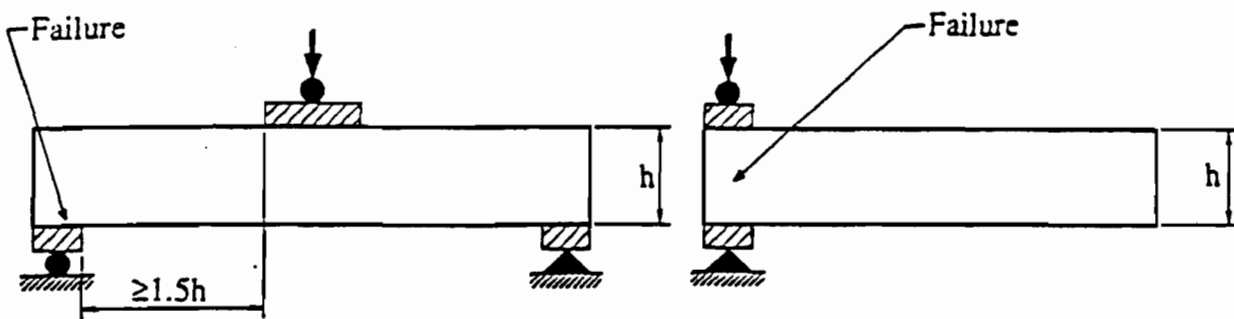
The first phase of Winter, Pian [4], and Zetlin's [14] research was the web crippling behavior of I-beams. These I-beams were categorized as beams which provided a high degree of restraint against rotation of the web. The results of these tests showed that the ultimate web crippling load of an I-beam depends primarily on the ratio  $N/t$  and the material yield strength,  $F_y$  [20], where  $N$  is defined to be the bearing length of the applied load in inches, and  $t$  is defined as the material thickness in inches. The second phase of Winter, Pian [4], and Zetlin's [14] study explored the behavior of cold-formed steel beams having single unreinforced webs, such as Z-sections, channels, and hat sections. It was found that the parameters controlling the web crippling strength for these sections were the ratios  $N/t$ ,  $R/t$ ,  $h/t$  and  $F_y$ , where  $R$  is defined to be the inside bend radius in inches, and  $h$  is defined as the clear distance between flanges measured along the plane of web in inches. The empirical expressions derived by Winter, Pian [4], and Zetlin's [14] study for predicting the web crippling strength for each type of section were incorporated into the 1968 AISI Specification [27].

Hetrakul and Yu [5] performed research at the University of Missouri-Rolla on the web crippling behavior of single and multiple web sections and their findings were used to modify the AISI Specification [28] design equations.



(a) Interior One-Flange Loading (IOF)

(c) Interior Two-Flange Loading (ITF)



(b) Exterior One-Flange Loading (EOF)

(d) Exterior Two-Flange Loading (ETF)

Figure 6. Web Crippling Loading Conditions [4, 7]

Also at the University of Missouri-Rolla, Santaputra and Yu [20] researched the web-crippling strength of high strength cold-formed steel beams and developed suggested prediction equations for web crippling capacities. These empirical equations distinguish between web crippling failure caused by local yielding failure and buckling failure. Santaputra's equations have been adopted for the 1986 Automotive Steel Design Manual [29] as an alternate design method.

The current design criteria of the AISI Specification [3], the analytically derived equations proposed by Prabakaran and Schuster [7], and the Santaputra, Parks, and Yu [8] equations are presented in detail in the next section. In Section IV, the computed web crippling capacity obtained by these equations were compared to the experimental web crippling data generated during this study.

#### D. CURRENT DESIGN APPROACHES

As previously discussed, the theoretical methods of analysis for web crippling are very complex. Therefore, equations presently used to predict the web crippling strength of cold formed steel beams are empirical equations. The following is a review of the web crippling equations used to compare with the experimental web crippling data.

1. AISI Specification [3]: The following design criteria is taken from the American Iron and Steel Institute, Cold-Formed Steel Design Manual, Specification for the Design of Cold-Formed Steel Structural Members [3].

All design equations for determining the allowable reactions and concentrated loads to prevent web crippling for Z-sections, I-beams, channels, hat sections, square or rectangular tubes, steel decks, and panels are given in Table I. These equations can only

be used for unreinforced flat webs having  $h/t \leq 200$ ,  $N/t \leq 210$ ,  $N/h \leq 3.5$ ,  $R/t \leq 6$  for beams,  $R/t \leq 7$  for decks, and  $45^\circ \leq \theta \leq 90^\circ$ . The concentrated loads and reactions shall not exceed the values of  $P_a$  given in Table I.  $P_a$  represents the concentrated load or reaction for one solid web connecting top and bottom flanges. For two or more webs,  $P_a$  shall be computed for each individual web and the results added to obtain the allowable load or reaction for the multiple web. Figure 7 shows the applications of the equations in Table I for different types of loading conditions.

It can be seen from Eqs. 8, 9, 11, 13, and 15 (Table I), beams having single unreinforced webs, that the web crippling capacity depends on the ratios of  $N/t$ ,  $h/t$ , and  $R/t$ , the web thickness  $t$ ,  $F_y$ , and the web inclination angle  $\theta$ . These design equations are based on a safety factor of 1.85. This safety factor for web crippling is used due to primarily the typical high variance found in web crippling analysis. [30]

From Eqs. 10, 12, 14, and 16 (Table I), I-beams which provide a high degree of restraint against rotation of the web, the web crippling capacity depends on the ratio  $N/t$  and  $F_y$ . These design equations are based on a factor of safety of 2.0. The use of a large safety factor is based on the fact that test results showed considerable scatter. [2]

2. Prabakaran and Schuster Equations [7]: Prabakaran and Schuster completed an extensive analysis of the web crippling capacity of cold-formed steel sections by using the available experimental data taken from many sources. The object of their study was to develop simplified equations to calculate the web crippling capacity of cold-formed steel sections. Based on the results of their research project, Prabakaran and Schuster recommended Eq. 17 for the design of I-sections, single web sections and multiple web sections (decks) [7].

Table I. ALLOWABLE STRENGTH ( $P_a$ )

		Shapes Having Single Webs		I-Sections or Similar Sections <sub>(1)</sub>
		Stiffened or Partially Stiffened Flanges	Unstiffened Flanges	Stiffened, Partially Stiffened and Unstiffened Flanges
Opposing Loads Spaced $> 1.5h_{(2)}$	End Reaction <sub>(3)</sub>	Eq. 8	Eq. 9	Eq. 10
	Interior Reaction <sub>(4)</sub>	Eq. 11	Eq. 11	Eq. 12
Opposing Loads Spaced $\leq 1.5h_{(5)}$	End Reactions <sub>(3)</sub>	Eq. 13	Eq. 13	Eq. 14
	Interior Reaction <sub>(4)</sub>	Eq. 15	Eq. 15	Eq. 16

Footnotes and Equation References to Table I:

- (1) I-sections made of two channels connected back to back or similar sections which provide a high degree of restraint against rotation of the web ( such as I-sections made by welding two angles to a channel).
- (2) At locations of one concentrated load or reaction acting either on the top or bottom flange, when the clear distance between the bearing edges of this and adjacent opposite concentrated loads or reactions is greater than  $1.5h$ .
- (3) For end reactions of beams or concentrated loads on the end of cantilevers when the distance from the edge of the bearing to the end of the beam is less than  $1.5h$ .

- (4) For reactions and concentrated loads when the distance from the edge of bearing to the end of the beam is equal to or greater than  $1.5h$ .
- (5) At locations of two opposite concentrated loads or of a concentrated load and an opposite reaction acting simultaneously on the top and bottom flanges, when the clear distance between their adjacent bearing edges is equal to or less than  $1.5h$ .

Equations for Table I:

$$t^2 k C_3 C_4 C_\theta [179 - 0.33(h/t)] [1 + 0.01(N/t)] \quad (\text{Eq. 8})$$

$$t^2 k C_3 C_4 C_\theta [117 - 0.15(h/t)] [1 + 0.01(N/t)] \quad (\text{Eq. 9})$$

When  $N/t > 60$ , the factor  $[1 + 0.01(N/t)]$  may be increased to  $[0.71 + 0.015(N/t)]$

$$t^2 F_y C_6 (5.0 + 0.63\sqrt{N/t}) \quad (\text{Eq. 10})$$

$$t^2 k C_1 C_2 C_\theta [291 - 0.40(h/t)] [1 + 0.007(N/t)] \quad (\text{Eq. 11})$$

When  $N/t > 60$ , the factor  $[1 + 0.007(N/t)]$  may be increased to  $[0.75 + 0.011(N/t)]$

$$t^2 F_y C_5 (0.88 + 0.12m) (7.50 + 1.63\sqrt{N/t}) \quad (\text{Eq. 12})$$

$$t^2 k C_3 C_4 C_\theta [132 - 0.31(h/t)] [1 + 0.01(N/t)] \quad (\text{Eq. 13})$$

$$t^2 F_y C_8 (0.64 + 0.31m) (5.0 + 0.63\sqrt{N/t}) \quad (\text{Eq. 14})$$

$$t^2 k C_1 C_2 C_\theta [417 - 1.22(h/t)] [1 + 0.0013(N/t)] \quad (\text{Eq. 15})$$

$$t^2 F_y C_7 (0.82 + 0.15m) (7.50 + 1.63\sqrt{N/t}) \quad (\text{Eq. 16})$$

- Where  $P_a$  = Allowable concentrated load or reaction per web, kips.
- $$C_1 = ( 1.22 - 0.22 k )$$
- $$C_2 = [ 1.06 - 0.06 ( R / t ) ] \leq 1.0$$
- $$C_3 = ( 1.33 - 0.33 k )$$
- $$C_4 = 0.50 < [ 1.15 - 0.15 ( R / t ) ] \leq 1.0$$
- $$C_5 = ( 1.49 - 0.53 k ) \geq 0.6$$
- $$C_6 = 1 + [ ( h / t ) / 750 ] \text{ when } h / t \leq 150$$
- $$= 1.20, \text{ when } h / t > 150$$
- $$C_7 = 1 / k , \text{ when } h / t \leq 66.5$$
- $$= [ 1.10 - ( h / t ) / 665 ] / k , \text{ when } h / t > 66.5$$
- $$C_8 = [ 0.98 - ( h / t ) / 865 ] / k$$
- $$C_\theta = 0.7 + 0.3 ( \theta / 90 )^2$$
- $F_y$  = design yield stress of the web, ksi.
- $h$  = depth of the flat portion of the web measured along the plane of the web, inches.
- $k$  =  $F_y(\text{ksi}) / 33$
- $m$  =  $t / 0.075$
- $t$  = web thickness, inches.
- $N$  = actual length of bearing, inches. For the case of two equal and opposite concentrated loads distributed over unequal bearing lengths, the smaller value of  $N$  shall be taken.
- $R$  = inside bend radius.
- $\theta$  = angle between plane of web and plane of bearing surface in degrees.



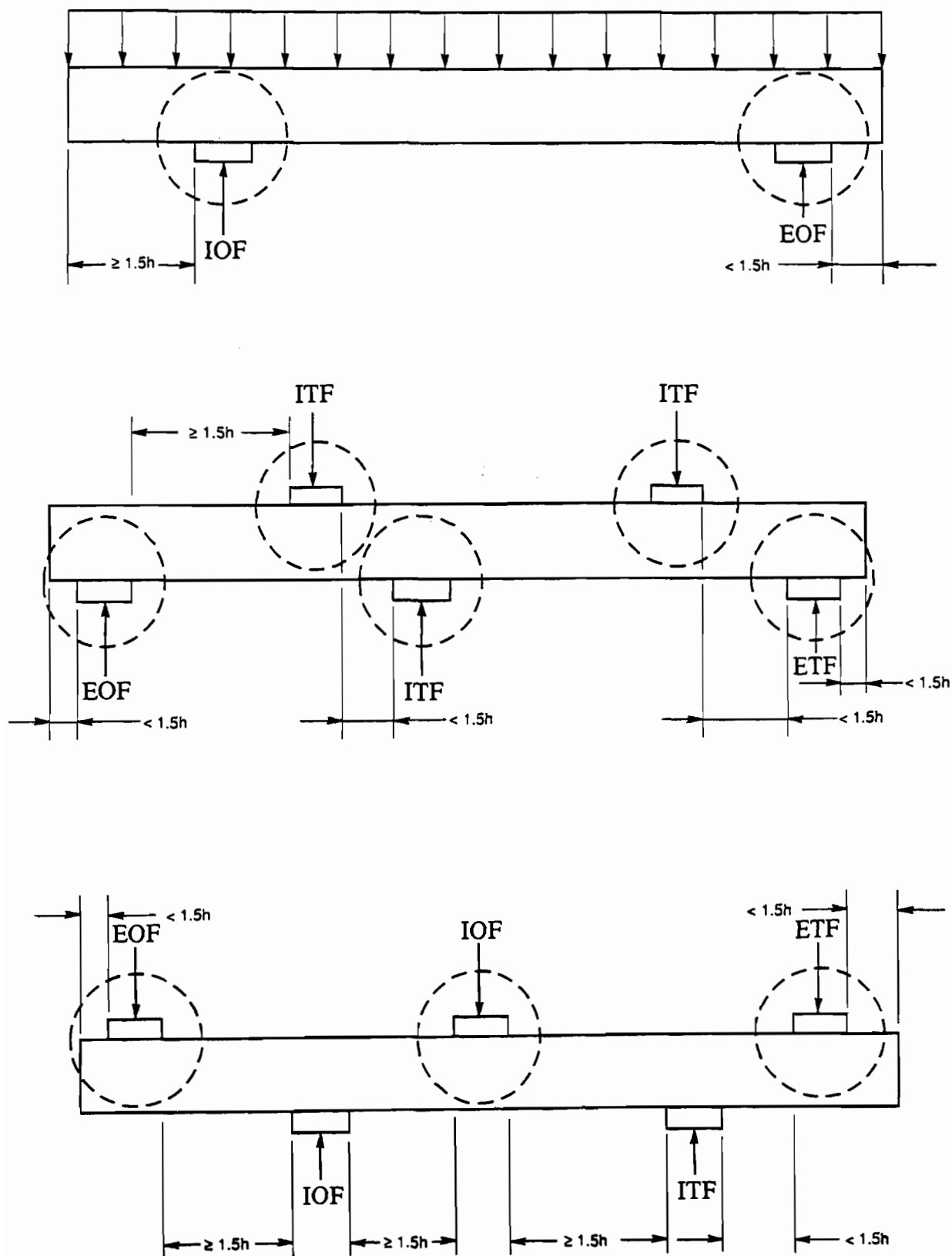


Figure 7. Application of Design Equations Listed in Table I [3]

$$P_n = C t^2 F_y (1 - C_R \sqrt{R}) (1 - C_N \sqrt{N}) (1 - C_H \sqrt{H}) \quad (\text{Eq. 17})$$

Table II summarizes the equation parameter coefficients. The parameter limits for I-sections and shapes having single webs are  $H \leq 200$ ,  $N \leq 200$ ,  $n/h \leq 1$  and  $R \leq 4$ , for multiple web sections (decks)  $H \leq 200$ ,  $N \leq 200$ ,  $n/h \leq 2$  and  $R \leq 10$ . [7] It should be noted that only few test data exceeded these limits, hence it is impossible to study the possibility of increasing the limits.

3. Santaputra, Parks, and Yu Equations [8]: Santaputra, Parks, and Yu developed additional design criteria for the use with a broader range of high-strength sheet steels. This study's recommended web crippling capacity equations were adopted by the Automotive Steel Design Manual [29].

The current AISI Specification [3] web crippling equations have distinct transitions between the EOF, IOF, ETF, and the ITF loading conditions. The equations provided by Santaputra, Parks, and Yu are derived from the test data obtained from the four basic loading conditions stated above. This allows their equations to be more versatile by allowing transitions between the one and two-flange loading conditions and the end and interior loading conditions. This is accomplished by using specific geometric parameters as variables in the equations. The variables chosen for their equations were  $Z$  and  $e$ , and are shown in Figure 8 for the EOF loading condition and in Figure 9 for the IOF loading condition.

The equations developed by Santaputra, Parks, and Yu [8] can be related to the basic four loading condition conventions of the AISI Specification [3] by determining the values of the parameters  $Z$  and  $e$  as shown in Figures 8 and 9. These values of  $Z$  and

Table II. RECOMMENDED EXPRESSION

$P_n = C t^2 F_y (1 - C_R \sqrt{R}) (1 + C_N \sqrt{N}) (1 - C_H \sqrt{H}) \quad (\text{Eq. 17})$					
$P_n = C t^2 F_y (\sin \theta) (1 - C_R \sqrt{R}) (1 + C_N \sqrt{N}) (1 - C_H \sqrt{H}) \quad (\text{Eq. 17}^*)$					
	Eq.	C	$C_R$	$C_N$	$C_H$
<b>I-SECTIONS</b>					
a) EOF	17	9.85	0.185	0.315	0.001
b) IOF	17	18.0	0.001	0.075	0.001
c) ETF	17	15.0	0.001	0.100	0.050
d) ITF	17	28.0	0.001	0.035	0.025
<b>SINGLE WEB SECTIONS</b>					
a) EOF					
i) Stiffened Flanges	17	4.00	0.230	0.650	0.035
ii) Unstiffened Flanges	17	7.20	0.250	0.120	0.030
b) IOF	17	17.0	0.130	0.130	0.040
c) ETF	17	17.0	0.400	0.064	0.045
d) ITF	17	29.5	0.135	0.080	0.060
<b>MULTIPLE WEB SECTIONS (DECKS)</b>					
a) EOF	17*	4.00	0.070	0.200	0.001
b) IOF	17*	21.0	0.120	0.065	0.040
c) ETF	17*	9.00	0.180	0.200	0.044
d) ITF	17*	10.0	0.140	0.210	0.020

Note: See Figure 6 for definition of EOF, IOF, ETF, and ITF.

Equation 17 applies to I-section and single web sections when  $R \leq 4$ ,  $N \leq 200$ ,  $H \leq 200$ , and  $n/h \leq 1$ .

Equation 17\* applies to multiple web sections when  $R \leq 10$ ,  $N \leq 200$ ,  $H \leq 200$ , and  $n/h \leq 2$ .

The following is a list of notations used in Eq. 9 of Table II:

- $P_n$  = nominal computed web crippling load or reaction per web, kips.
- $C$  = coefficient.
- $C_H$  = web slenderness coefficient.
- $C_N$  = bearing length coefficient.
- $C_R$  = inside bend radius coefficient.
- $F_y$  = yield strength of steel, ksi.
- $H$  = web slenderness ratio,  $h/t$ .
- $h$  = depth of flat portion of the web measured in the plane of the web, in.
- $N$  = bearing length to web thickness ratio,  $n/t$ .
- $n$  = actual bearing length, inches. When two equal and opposite loads are distributed over unequal bearing lengths, use the smaller value of  $n$ .
- $R$  = inside bend radius to thickness ratio,  $r/t$ .
- $r$  = inside bend radius, in.
- $t$  = web thickness.
- $\theta$  = angle between the plane of the web and the plane of the bearing surface  $\geq 45^\circ$ , but not more than  $90^\circ$ .

$e$  can be correlated to the EOF, IOF, ETF, and ITF loading conditions as follows. For the end loading conditions, EOF and ETF, the  $Z$  value is less than  $1.5h$ . An  $e$  value greater than  $1.5h$  is considered to be an EOF loading condition. An  $e$  value less than or equal to  $1.5h$  is taken as an ETF loading condition. For the interior loading conditions, IOF and ITF, the  $Z$  value is greater than or equal to  $1.5h$ . An  $e$  value greater than  $1.5h$

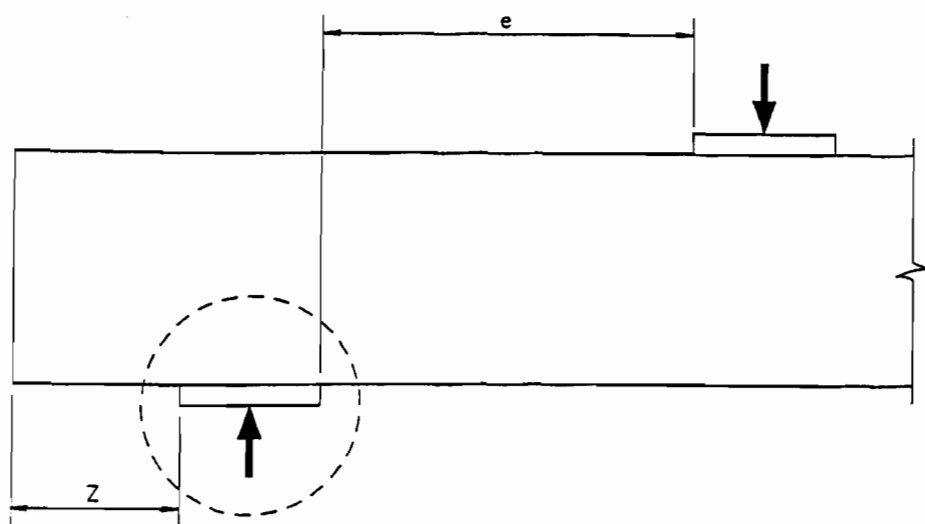


Figure 8. Santaputra, Parks and Yu Web Crippling Equation Parameter Definitions for EOF Loading Condition

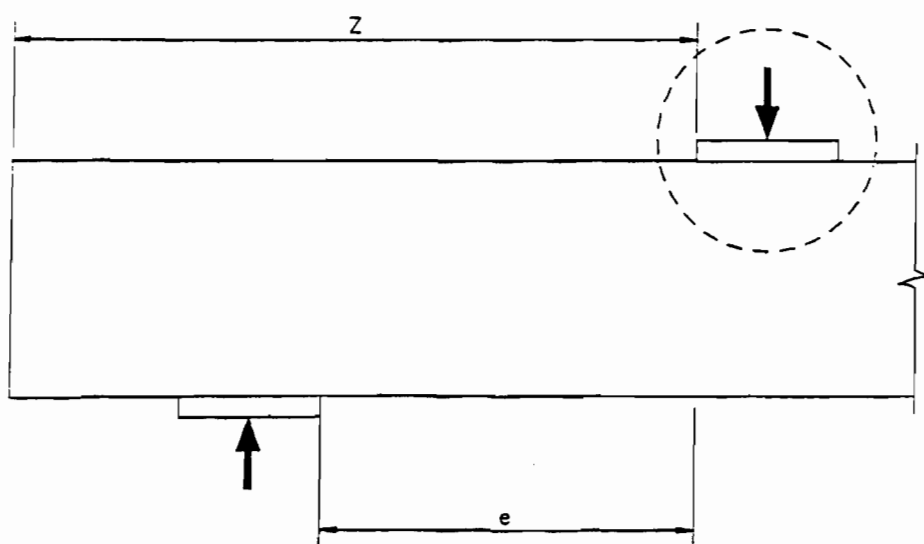


Figure 9. Santaputra, Parks and Yu Web Crippling Equation Parameter Definitions for IOF Loading Condition

is an IOF loading condition. An  $e$  value less than or equal to  $1.5h$  is an ITF loading condition. These correlations can be seen in Figures 8 and 9 for Santaputra, Parks, and Yu [8] parameters and in Figure 7 for AISI Specification [3] parameters.

The strength equations of Santaputra, Parks, and Yu [8] that are applicable to this investigation are Eqs. 18 to 21. The respective parameter limits for Eqs. 18 to 21 are  $h/t \leq 200$ ,  $N/t \leq 100$ ,  $N/h \leq 2.5$ ,  $R/t \leq 10$ , and  $F_y \leq 190$  ksi. For single unreinforced webs exposed to an EOF loading condition and having  $Z = 0$  and  $e \geq 1.5h$  the nominal web crippling load,  $P_n$ , is equal to the lesser of  $P_{cy}$  and  $P_{cb}$ .

$$P_{cy} = 9.9 t^2 F_y C_{11} C_{21} (\sin \theta) \quad (\text{Eq. 18})$$

$$P_{cb} = 0.047 E t^2 C_{41} C_{51} (\sin \theta) \quad (\text{Eq. 19})$$

For I-beams experiencing an IOF loading condition and with  $Z \geq .5h$  and  $e \geq 1.5h$ ,  $P_n$  is equal to the lesser of  $P_{cy}$  and  $P_{cb}$ .

$$P_{cy} = 15 t^2 F_y C_{12} \quad (\text{Eq. 20})$$

$$P_{cb} = 0.032 E t^2 C_{36} C_{46} \quad (\text{Eq. 21})$$

Where  $P_{cy}$  = the ultimate web crippling load caused by bearing, per web, kips.  
 $P_{cb}$  = the ultimate web crippling load caused by buckling, per web, kips.  
 $C_{11} = 1 + 0.0122 (N/t) \leq 2.22$   
 $C_{12} = 1 + 0.217 \sqrt{(N/t)} \leq 3.17$   
 $C_{21} = 1 - 0.247 (R/t) \geq 0.32$   
 $C_{36} = 1 + 1.318 (N/h) \leq 1.53$

$$C_{41} = 1 - 0.00348 (h / t) \geq 0.32$$

$$C_{46} = 1 - 0.000471 (h / t) \leq 0.95$$

$$C_{51} = 1 - 0.298 (e / h) \geq 0.52$$

$F_y$  = yield strength of the web material, ksi.

$E$  = modulus of elasticity of steel, 29500 ksi.

$t$  = web thickness, in.

$h$  = depth of the flat portion of the web, in.

$N$  = length of bearing, in.

$R$  = inside bend radius, in.

$e$  = defined in Figures 8 and 9

$Z$  = defined in Figures 8 and 9

$\theta$  = angle between the plane of the web and the plane of the bearing surface  $\geq 45^\circ$ , but not more than  $90^\circ$ .

### III. EXPERIMENTAL INVESTIGATION

#### A. GENERAL

As stated in Section I, the current design criteria for determining web crippling strength of cold-formed steel members is primarily based on test results in which the flanges were not fastened to the support beam. This support condition may not represent accurate field practices used in some situations. In some cases, the flanges of sections are not fastened to the support members, and the existing AISI Specification equations estimate the web crippling strength accurately. But, in other cases, the flanges are either bolted or welded to the support members. Due to the restraining affect of the fasteners, the AISI Specification equations may underestimate the web crippling strength of the member. Therefore, this study was initiated in 1994 and sponsored by the American Iron and Steel Institute (AISI), and the Metal Building Manufacture's Association (MBMA) to further study the web crippling capacity of Z- and I- section members with their flanges fastened to supports.

The objective of this experimental investigation was to explore the potential conservative and unconservative aspects of the present design provisions for web crippling of Z- and I-sections. This phase of the investigation focused only on the end one-flange loading (EOF) condition of Z-sections to further study the web crippling capacity of the Z-section members with their flanges fastened to the support. This study also focused only on the interior one-flange loading (IOF) condition of back-to-back C-sections to form I-sections to study the web crippling strength due to the bolt configuration used to inter-connect the sections together. It is intended to use the



research findings to develop suggested design modifications for web crippling strength of Z-sections subjected to an EOF loading condition.

This study consisted of 42 tests of cold-formed steel Z- and I-sections as summarized in Table III. The EOF loading condition was used for testing the 28 Z-sections. The IOF loading condition was used when testing the 14 I-sections. The results of these tests were used to evaluate the accuracy of the current design equations for web crippling strength.

All tests were performed using the 120,000 pound Tinius Olson universal testing machine (Figure 10) located in the Engineering Research Laboratory of the University of Missouri-Rolla. All test specimens were made from cold-formed steel sections and the supporting beams and load beam were hot-rolled I-beams.

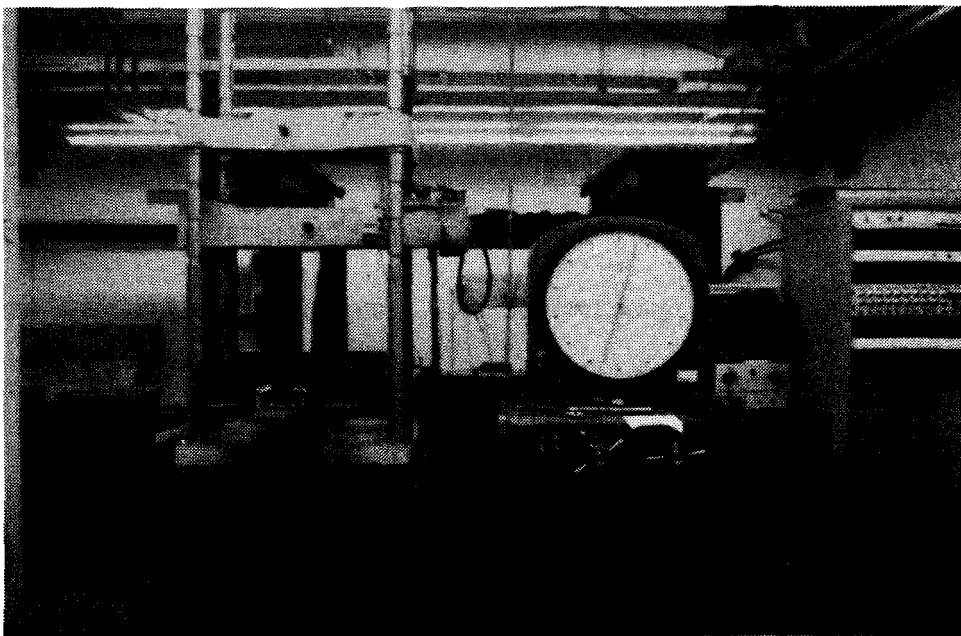


Figure 10. Tinius Olson Universal Testing Machine

Table III. TEST PROGRAM

Section Type	h/t	Number of Tests		Total	
		Unfastened Flanges	Fastened Flanges		
Z-Sections :	Z1	96	2	2	4
	Z2	70	2	2	4
	Z3	129	2	2	4
	Z4	94	2	2	4
	Z5	150	2	2	4
	Z6	118	2	2	4
	Z7	143	2	2	4
I-Sections :	I1	112	1	6	7
	I2	89	1	6	7
Total:					42

During the experimental phase of this investigation, the mechanical properties and thicknesses of all test specimens were determined. Table IV gives the average values of these mechanical properties and thicknesses. The mechanical properties were determined by Standard Coupon Tests per ASTM A370 procedures [31].

## B. TEST SPECIMENS

The test specimens used in this study were cold-formed steel Z- and I-sections. The cross-sectional view of the Z-section is shown in Figure 11, and the cross-sectional

Table IV. MATERIAL PROPERTIES AND THICKNESSES OF SECTIONS USED IN THE EXPERIMENTAL STUDIES

Section Type		t (in.)	F <sub>y</sub> (ksi)	F <sub>u</sub> (ksi)	Elongation (%) *
Z-Sections :	Z1	.061	61.75	84.26	32.82
	Z2	.083	65.19	86.27	27.08
	Z3	.061	62.03	89.18	31.25
	Z4	.083	63.05	78.98	29.69
	Z5	.059	73.11	88.99	25.78
	Z6	.075	73.78	88.67	25.00
	Z7	.075	56.89	78.22	31.77
I-Sections :	I1	.067	61.20	79.35	34.38
	I2	.085	63.34	80.00	28.91

\* Elongation was measured over a 2-in. gage length

view of the I-beam is shown in Figure 12. The nominal cross-section dimensions of the tested sections were measured from photocopies of the cross-sectional views of each specimen. These cross-section dimensions are located in Tables V and VI. The specimens were cut to length from 20 to 25 feet long sections by using a 14 inch diameter chop saw. The process of cutting short sections from longer section releases residual stresses in the specimens. These residual stresses caused some minor twisting, but did not influence the results of the tests. The length of beam specimens were selected so that only the effect of web crippling occurred, not the combination of web

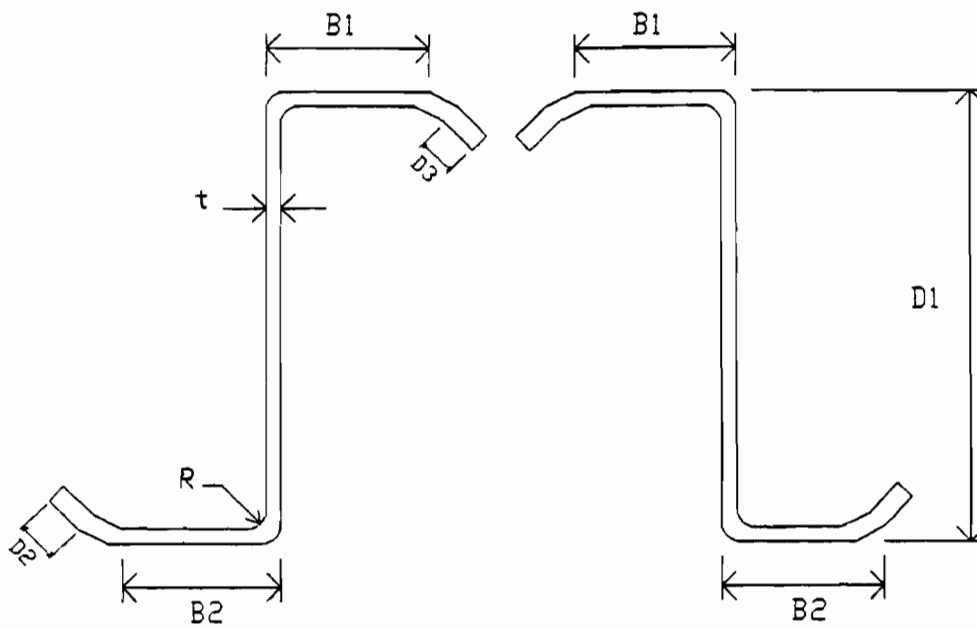


Figure 11. Cross Section View of a Z-Section Specimen [6]

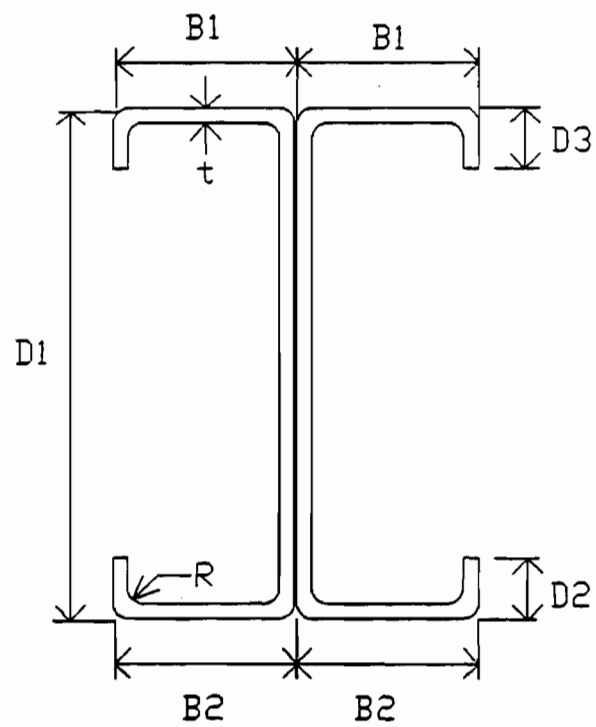


Figure 12. Cross Section View of an I-Beam Specimen [6]

**Table V. MEASURED DIMENSIONS OF Z-SECTIONS**

<b>Specimen No.</b>	<b>t (in.)</b>	<b>B1 (in.)</b>	<b>B2 (in.)</b>	<b>D1 (in.)</b>	<b>D2 (in.)</b>	<b>D3 (in.)</b>	<b>R (in.)</b>	<b>N (in.)</b>	<b>L (in.)</b>
Z1.1	0.061	1.656	1.750	6.469	0.406	0.406	0.250	2.625	30.000
Z1.2	0.061	1.625	1.719	6.453	0.438	0.438	0.250	2.625	30.000
Z1.3-F	0.061	1.689	1.781	6.469	0.406	0.438	0.250	2.625	30.000
Z1.4-F	0.061	1.688	1.750	6.453	0.406	0.406	0.250	2.625	30.000
Z2.1	0.083	1.656	1.813	6.469	0.438	0.438	0.250	2.625	30.000
Z2.2	0.083	1.688	1.656	6.469	0.469	0.469	0.250	2.625	30.000
Z2.3-F	0.083	1.656	1.719	6.469	0.406	0.438	0.250	2.625	30.000
Z2.3-F	0.083	1.688	1.719	6.469	0.469	0.469	0.250	2.625	30.000

**Note:** Refer to Figure 11 for Definitions

**Table V (Cont'd.). MEASURED DIMENSIONS OF Z-SECTIONS**

<b>Specimen No.</b>	<b>t (in.)</b>	<b>B1 (in.)</b>	<b>B2 (in.)</b>	<b>D1 (in.)</b>	<b>D2 (in.)</b>	<b>D3 (in.)</b>	<b>R (in.)</b>	<b>N (in.)</b>	<b>L (in.)</b>
<b>Z3.1</b>	0.061	2.250	2.344	8.469	0.531	0.531	0.250	2.625	36.000
<b>Z3.2</b>	0.061	2.250	2.375	8.484	0.563	0.563	0.250	2.625	36.000
<b>Z3.3-F</b>	0.061	2.250	2.344	8.469	0.563	0.563	0.250	2.625	36.000
<b>Z3.4-F</b>	0.061	2.250	2.375	8.484	0.531	0.563	0.250	2.625	36.000
<b>Z4.1</b>	0.083	2.189	2.375	8.484	0.641	0.641	0.250	2.625	36.000
<b>Z4.2</b>	0.083	2.250	2.344	8.484	0.689	0.689	0.250	2.625	36.000
<b>Z4.3-F</b>	0.083	2.250	2.375	8.500	0.689	0.656	0.250	2.625	36.000
<b>Z4.4-F</b>	0.083	2.250	2.375	8.500	0.689	0.656	0.250	2.625	36.000

**Note:** Refer to Figure 11 for Definitions

**Table V (Cont'd.). MEASURED DIMENSIONS OF Z-SECTIONS**

<b>Specimen No.</b>	<b>t (in.)</b>	<b>B1 (in.)</b>	<b>B2 (in.)</b>	<b>D1 (in.)</b>	<b>D2 (in.)</b>	<b>D3 (in.)</b>	<b>R (in.)</b>	<b>N (in.)</b>	<b>L (in.)</b>
<b>Z5.1</b>	0.059	2.438	2.438	9.500	0.484	0.500	0.250	2.625	39.000
<b>Z5.2</b>	0.059	2.438	2.469	9.484	0.469	0.484	0.250	2.625	39.000
<b>Z5.3-F</b>	0.059	2.438	2.438	9.500	0.484	0.500	0.250	2.625	39.000
<b>Z5.4-F</b>	0.059	2.438	2.469	9.484	0.469	0.500	0.250	2.625	39.000
<b>Z6.1</b>	0.075	2.469	2.484	9.484	0.719	0.781	0.250	2.625	39.000
<b>Z6.2</b>	0.075	2.438	2.469	9.500	0.734	0.750	0.250	2.625	39.000
<b>Z6.3-F</b>	0.075	2.469	2.484	9.484	0.719	0.781	0.250	2.625	39.000
<b>Z6.4-F</b>	0.075	2.438	2.469	9.500	0.714	0.750	0.250	2.625	39.000

**Note: Refer to Figure 11 for Definitions**

**Table V (Cont'd.). MEASURED DIMENSIONS OF Z-SECTIONS**

<b>Specimen No.</b>	<b>t (in.)</b>	<b>B1 (in.)</b>	<b>B2 (in.)</b>	<b>D1 (in.)</b>	<b>D2 (in.)</b>	<b>D3 (in.)</b>	<b>R (in.)</b>	<b>N (in.)</b>	<b>L (in.)</b>
<b>Z7.1</b>	<b>0.075</b>	<b>3.172</b>	<b>3.375</b>	<b>11.516</b>	<b>0.609</b>	<b>0.672</b>	<b>0.313</b>	<b>2.625</b>	<b>45.000</b>
<b>Z7.2</b>	<b>0.075</b>	<b>3.186</b>	<b>3.391</b>	<b>11.500</b>	<b>0.609</b>	<b>0.672</b>	<b>0.313</b>	<b>2.625</b>	<b>45.000</b>
<b>Z7.3-F</b>	<b>0.075</b>	<b>3.172</b>	<b>3.375</b>	<b>11.516</b>	<b>0.609</b>	<b>0.672</b>	<b>0.313</b>	<b>2.625</b>	<b>45.000</b>
<b>Z7.4-F</b>	<b>0.075</b>	<b>3.186</b>	<b>3.391</b>	<b>11.500</b>	<b>0.609</b>	<b>0.672</b>	<b>0.313</b>	<b>2.625</b>	<b>45.000</b>

**Note: Refer to Figure 11 for Definitions**



**Table VI. MEASURED DIMENSIONS OF I-SECTIONS**

<b>Specimen No.</b>	<b>t (in.)</b>	<b>B1 (in.)</b>	<b>B2 (in.)</b>	<b>D1 (in.)</b>	<b>D2 (in.)</b>	<b>D3 (in.)</b>	<b>R (in.)</b>	<b>N (in.)</b>	<b>L (in.)</b>
I1	0.067	2.609	2.531	7.953	0.984	0.859	0.156	5.250	39.750
I1-F	0.067	2.609	2.531	7.953	0.984	0.859	0.156	5.250	39.750
I2-F	0.067	2.625	2.516	7.921	1.000	0.875	0.156	5.250	39.750
I3-F	0.067	2.609	2.516	7.938	0.984	0.875	0.156	5.250	39.750
I4-F	0.067	2.609	2.531	7.921	1.000	0.859	0.156	5.250	39.750
I5-F	0.067	2.625	2.531	7.938	1.000	0.859	0.156	5.250	39.750
I6-F	0.067	2.625	2.516	7.953	0.984	0.875	0.156	5.250	39.750
I7	0.085	2.406	2.656	8.063	0.984	0.906	0.156	5.250	39.750
I7-F	0.085	2.406	2.656	8.063	0.984	0.906	0.156	5.250	39.750
I8-F	0.085	2.422	2.641	8.000	1.000	0.922	0.156	5.250	39.750
I9-F	0.085	2.406	2.641	7.984	0.984	0.906	0.156	5.250	39.750
I10-F	0.085	2.422	2.656	8.000	0.984	0.922	0.156	5.250	39.750
I11-F	0.085	2.422	2.641	7.984	1.000	0.922	0.156	5.250	39.750
I12-F	0.085	2.406	2.656	8.063	1.000	0.906	0.156	5.250	39.750

Note: Refer to Figure 12 for Definitions

cripling and bending. The equations used to determine the length,  $L$  in inches, of the test specimens for the EOF and IOF loading conditions are as follows: [6]

EOF Loading Condition:

$$L = 2(1.5h) + 2N + 5.25 \quad (\text{Eq. 22})$$

IOF Loading Condition:

$$L = 2(1.5h) + N + 10.5 \quad (\text{Eq. 23})$$

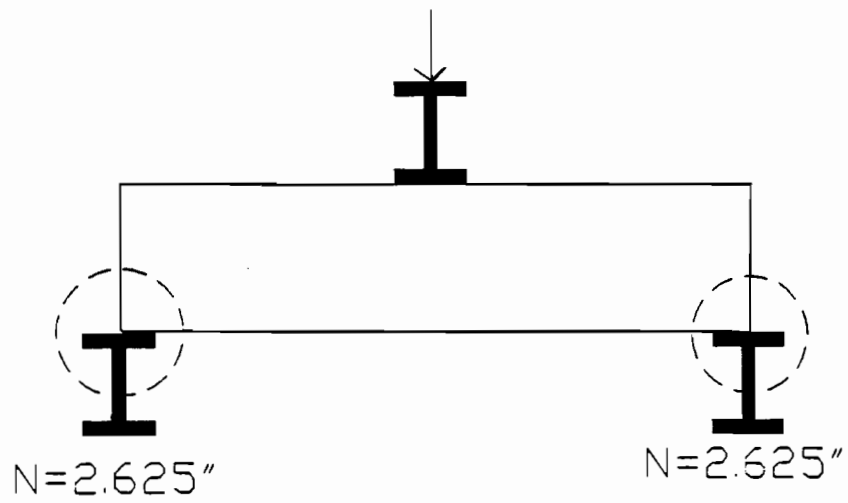
where,  $h$  = flat width of the web, inches.

$N$  = bearing length, inches.

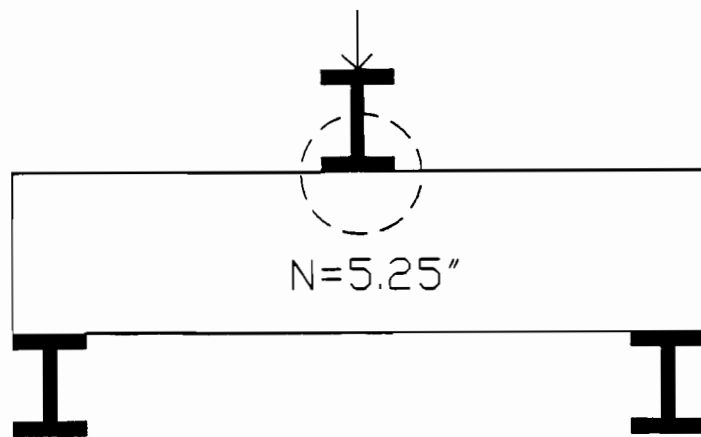
Figure 13 shows the typical bearing conditions for the EOF and IOF loading conditions. The distance between the support and the load bearing edges was kept slightly greater than  $1.5h$  to maintain a one-flange loading condition (Figure 14).

In order to cause EOF and IOF type failures, stiffeners were added to the specimens at specific locations. For the case of the EOF loading condition, the portion of the web directly under the concentrated load was stiffened to force the failure to occur at the ends. For the case of the IOF loading condition, the portion of the web directly above the end supports was stiffened to force the failure to occur directly under the interior concentrated load. The EOF and IOF loading condition stiffener locations are shown in Figure 14.

As stated previously, a total of 42 tests were performed for the EOF and IOF loading conditions. The EOF loading condition was used when testing the 28 Z-sections.

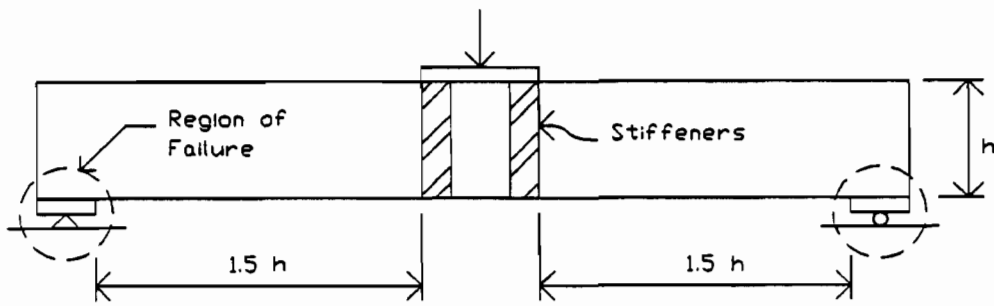


(a) EOF Loading Condition

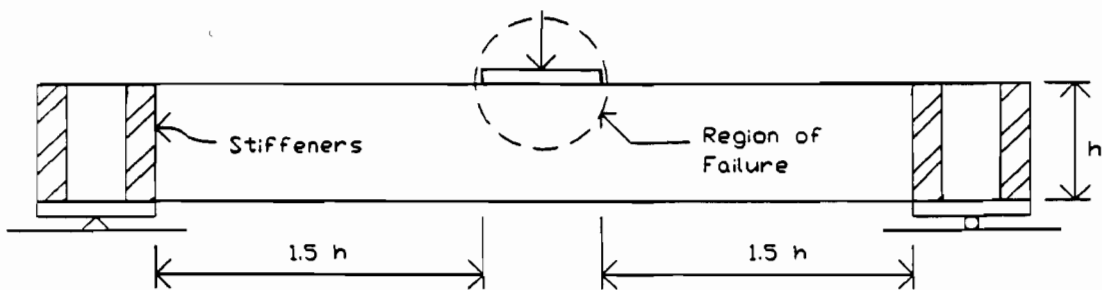


(b) IOF Loading Condition

Figure 13. Typical Bearing Conditions for EOF and IOF Loading Conditions [6]



(a) EOF Loading Condition



(b) IOF Loading Condition

Figure 14. EOF and IOF Loading Condition Stiffener Locations [6]

One half of these Z-sections were tested with the flanges fastened to the support, and the other half were tested with the flanges not fastened to the supports. The IOF loading condition was used for testing the 14 I-sections. Twelve of the I-sections were tested with the flanges fastened to the supports, and two were tested with the flanges not fastened to the support. The fasteners used for restraining the flanges were 1/2 inch diameter A325T bolts. These fasteners connected the flanges of the cold-formed steel section being tested to the supporting I-beams. For the EOF loading condition, the end flanges of the fastened flange Z-sections were attached to the end supporting I-beams. For the IOF loading condition, both flanges below the concentrated load of the I-beam were fastened to the load beam.

The important test data parameters used in the strength calculations are given in Tables VII and VIII.

### C. TEST PROCEDURES

All specimens were loaded to failure. The details of the test arrangement for the Z-sections and I-sections for each loading condition are summarized as follows:

1. Z-Sections: A total of 28 Z-section specimens were tested, half of which were tested with the flanges fastened to the support, and the other half was tested with the flanges unfastened to the supports. The EOF loading condition was used to test the Z-section specimens. These sections were tested as simply supported members subjected to a concentrated load applied at the mid-span. The member length was chosen to provide a minimum of  $1.5h$  distance between the edges of bearing plates. This length was calculated by using Eq. 22.

Table VII. EQUATION PARAMETERS AND TEST DATA OF Z-SECTIONS

Specimen No.	t (in.)	h/t	R/t	N/t	N/h	F <sub>y</sub> (ksi)	P <sub>t</sub> (kips)
Z1.1	0.061	95.852	4.098	43.033	0.449	61.750	1.036
Z1.2	0.061	95.590	4.098	43.033	0.450	61.750	0.993
Z1.3-F	0.061	95.852	4.098	43.033	0.449	61.750	1.575
Z1.4-F	0.061	95.590	4.098	43.033	0.450	61.750	1.570
Z2.1	0.083	69.916	3.012	31.627	0.452	65.190	2.056
Z2.2	0.083	69.916	3.012	31.627	0.452	65.190	2.036
Z2.3-F	0.083	69.916	3.012	31.627	0.452	65.190	3.099
Z2.4-F	0.083	69.916	3.012	31.627	0.452	65.190	3.093
Z3.1	0.061	128.639	4.098	43.033	0.335	62.030	1.261
Z3.2	0.061	128.885	4.098	43.033	0.334	62.030	1.205
Z3.3-F	0.061	128.639	4.098	43.033	0.335	62.030	1.703
Z3.4-F	0.061	128.885	4.098	43.033	0.334	62.030	1.745
Z4.1	0.083	94.193	3.012	31.627	0.336	63.050	1.955
Z4.2	0.083	94.193	3.012	31.627	0.336	63.050	2.011
Z4.3-F	0.083	94.386	3.012	31.627	0.335	63.050	2.766
Z4.4-F	0.083	94.386	3.012	31.627	0.335	63.050	2.725

F = Represents specimens having flanges fastened to supports.

P<sub>t</sub> = Tested load per web.

N = 2.625 in.

Table VII (Cont'd.). EQUATION PARAMETERS AND TEST DATA OF Z-SECTIONS

Specimen No.	t (in.)	h/t	R/t	N/t	N/h	F <sub>y</sub> (ksi)	P <sub>t</sub> (kips)
Z5.1	0.059	150.542	4.237	44.492	0.296	73.110	1.328
Z5.2	0.059	150.271	4.237	44.492	0.296	73.110	1.319
Z5.3-F	0.059	150.542	4.237	44.492	0.296	73.110	1.406
Z5.4-F	0.059	150.271	4.237	44.492	0.296	73.110	1.396
Z6.1	0.075	117.787	3.333	35.000	0.297	73.780	1.327
Z6.2	0.075	118.000	3.333	35.000	0.297	73.780	1.303
Z6.3-F	0.075	117.787	3.333	35.000	0.297	73.780	1.353
Z6.4-F	0.075	118.000	3.333	35.000	0.297	73.780	1.328
Z7.1	0.075	143.200	4.173	35.000	0.244	56.890	1.524
Z7.2	0.075	142.987	4.173	35.000	0.245	56.890	1.529
Z7.3-F	0.075	143.200	4.173	35.000	0.244	56.890	2.024
Z7.4-F	0.075	142.987	4.173	35.000	0.245	56.890	2.050

F = Represents specimens having flanges fastened to supports.

P<sub>t</sub> = Tested load per web.

N = 2.625 in.

The Z-section specimens were fabricated by connecting two sections together with 3/4 X 3/4 X 1/8 inch aluminum angles at a specified bracing interval. The interval was selected so as to minimize lateral movement between the two sections. Therefore, the aluminum angles were placed at 1/4 point locations from the ends of the test specimens

Table VIII. EQUATION PARAMETERS AND TEST DATA OF I-SECTIONS

Specimen No.	t (in.)	h/t	R/t	N/t	N/h	F <sub>y</sub> (ksi)	P <sub>t</sub> (kips)
I1	0.067	112.045	2.328	78.358	0.699	61.200	5.935
I1-F	0.067	112.045	2.328	78.358	0.699	61.200	6.048
I2-F	0.067	111.567	2.328	78.358	0.702	61.200	6.010
I3-F	0.067	111.821	2.328	78.358	0.701	61.200	6.223
I4-F	0.067	111.567	2.328	78.358	0.702	61.200	6.060
I5-F	0.067	111.821	2.328	78.358	0.701	61.200	6.173
I6-F	0.067	112.045	2.328	78.358	0.699	61.200	6.285
I7	0.085	89.188	1.835	61.765	0.693	63.340	9.788
I7-F	0.085	89.188	1.835	61.765	0.693	63.340	10.285
I8-F	0.085	88.447	1.835	61.765	0.698	63.340	10.060
I9-F	0.085	88.259	1.835	61.765	0.700	63.340	9.998
I10-F	0.085	88.447	1.835	61.765	0.698	63.340	9.985
I11-F	0.085	88.259	1.835	61.765	0.700	63.340	10.610
I12-F	0.085	89.188	1.835	61.765	0.693	63.340	10.285

F = Represents specimens having flanges fastened to supports.

P<sub>t</sub> = Tested load per web.

N = 5.25 in.



on the top, or compression side of the specimen. On the bottom, or tension side of the test specimen, an aluminum angle was placed at the mid-span location.

Before the specimens were connected together, small cold-formed steel channels, which served as transverse web stiffeners, were attached to the web. For the case of EOF loading condition, the portion of the web directly under the concentrated load was stiffened to force the failure to occur at the ends. The stiffener locations are shown in Figure 14.

Also, it was found that upon loading a 9.5 inch deep section that the webs were not stiff enough to keep the specimen from toppling over under load. Therefore, the 9.5 and 11.5 inch deep sections had additional cross bracing added at 1/4 point locations from the ends for lateral support during loading. The bracing used was 3/4 inch aluminum perforated tape, commonly called plumbers strapping tape. Lengths of this tape were fastened to the top 1/4 point location of one specimen's web with a self taping screw and stretched to the other specimen's bottom flange and fastened with another self taping screw. This cross bracing is shown in Figures 15 and 16.

The fasteners used for attaching the flanges to the supports were 1/2 inch diameter A325T bolts. The end flanges of the fastened flange Z-sections were attached to the end supporting I-beams. For all Z-sections tested, a 2-5/8 inch bearing length was used for the end supports and a 5-1/4 inch bearing length was used under the interior applied concentrated load. See Figures 15, 16, 17 and 18 for the test specimen fabrication of the unfastened and the fastened flange Z-sections subjected to EOF loading condition.

2. I-Sections: A total of 14 I-section test specimens were tested and subjected to the IOF loading condition. Twelve of which were tested with the flanges fastened to

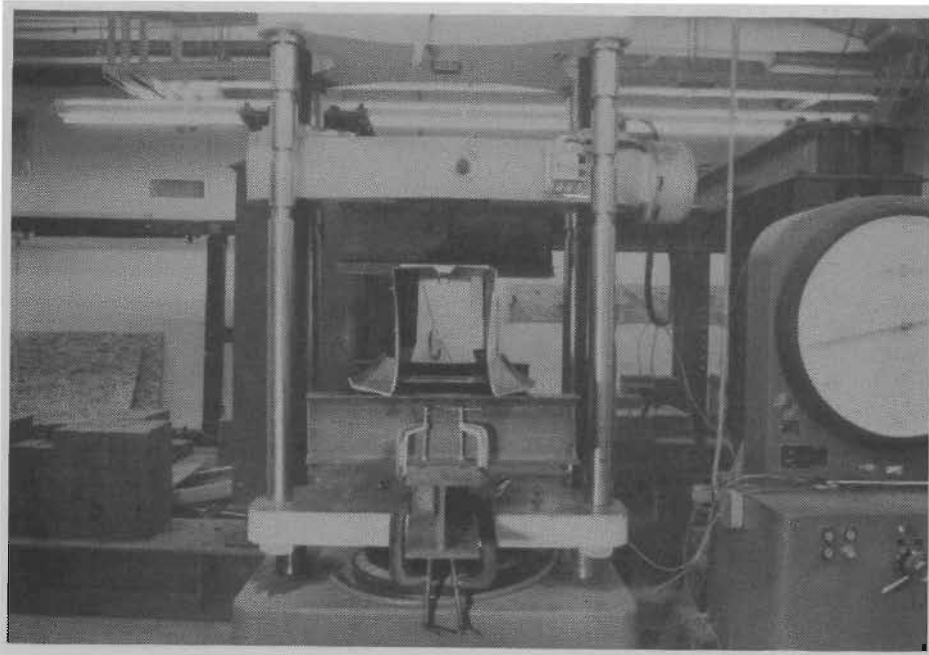


**Figure 15.** Photograph of Typical Failure of a Z-Section with Cross-Bracing Subjected to EOF Loading Condition with Unrestrained Flanges

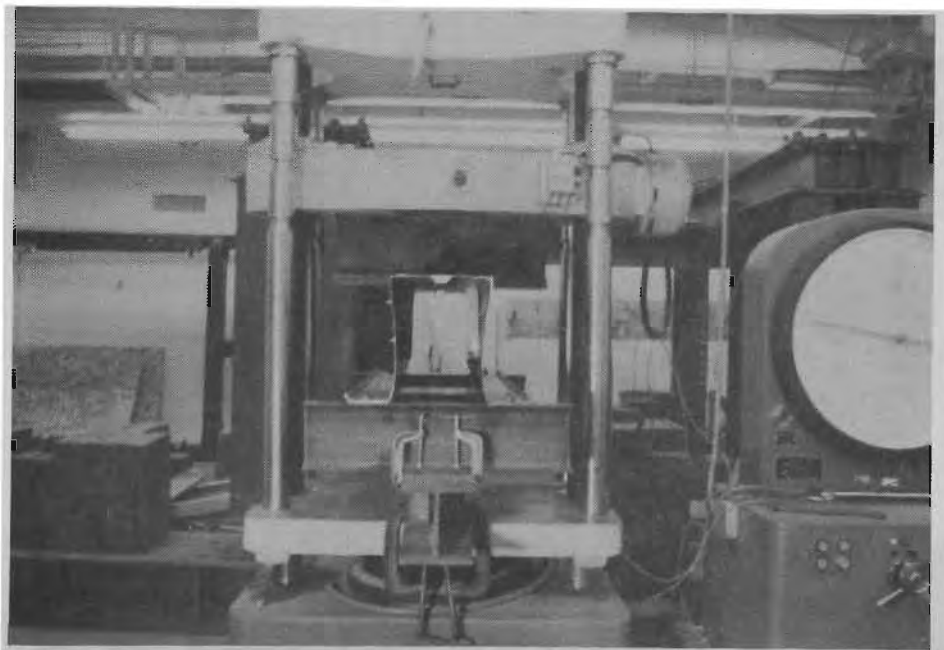


**Figure 16.** Photograph of Typical Failure of a Z-Section with Cross-Bracing Subjected to EOF Loading Condition with Restrained Flanges

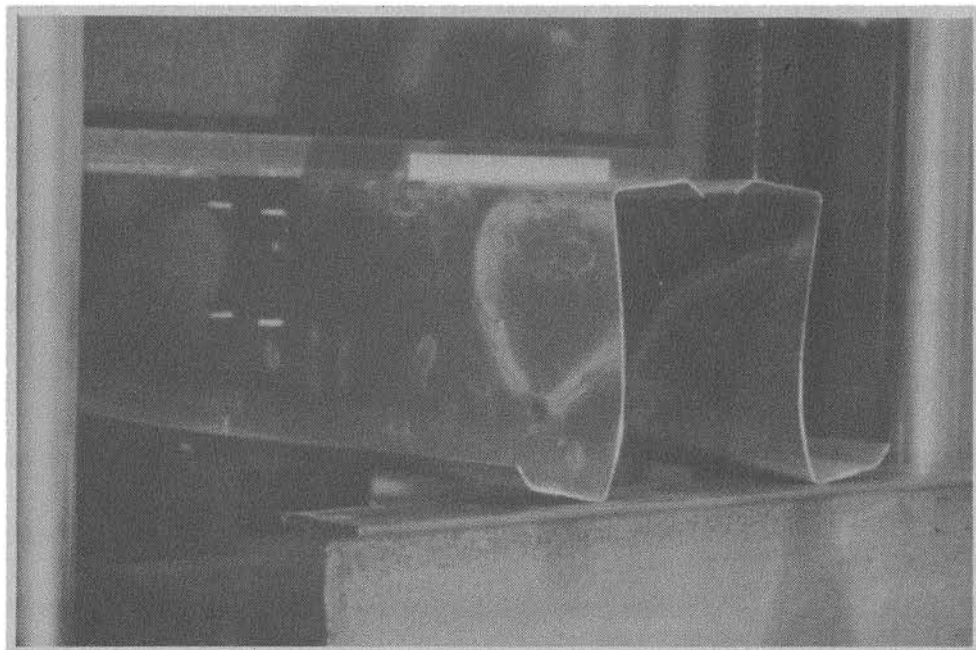


**Figure 17.** Photograph of a Typical Failure of Z-Section Subjected to EOF Loading Condition with Unrestrained Flanges

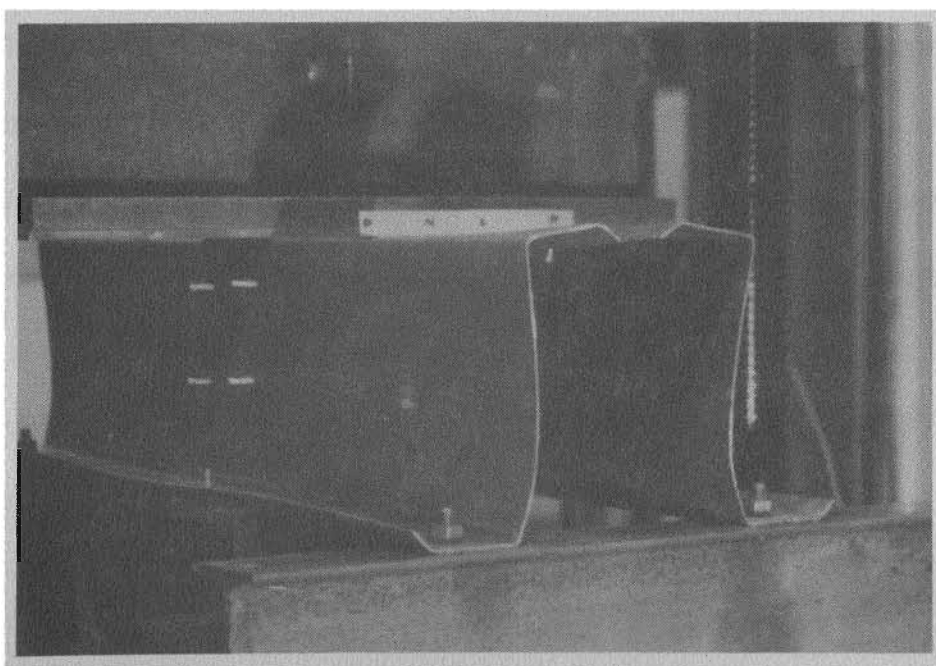


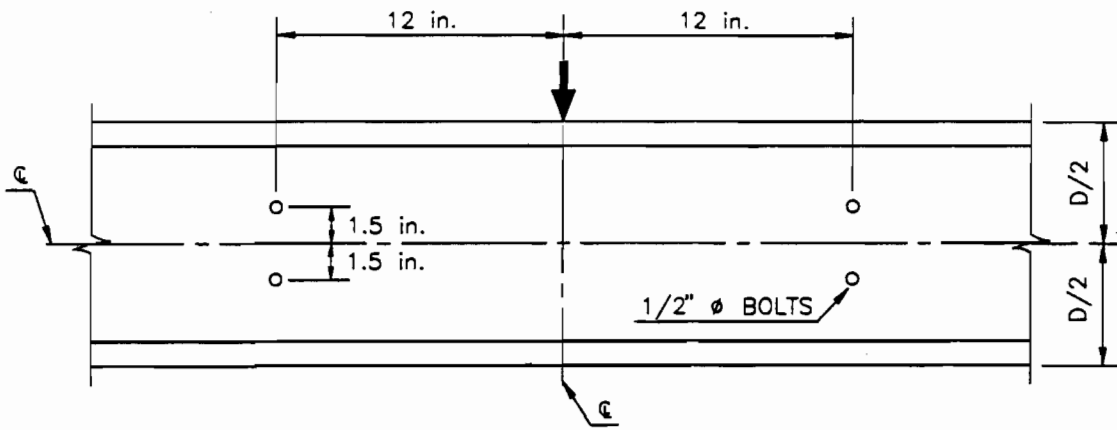
**Figure 18.** Photograph of a Typical Failure of Z-Section Subjected to EOF Loading Condition with Restrained Flanges

the supports, and two were tested with the flanges unfastened. These sections were tested as simply supported members subjected to a concentrated load applied at mid-span. The member length was chosen to provide a minimum of  $1.5h$  distance between the edges of bearing plates. The length was calculated by using Eq. 23.

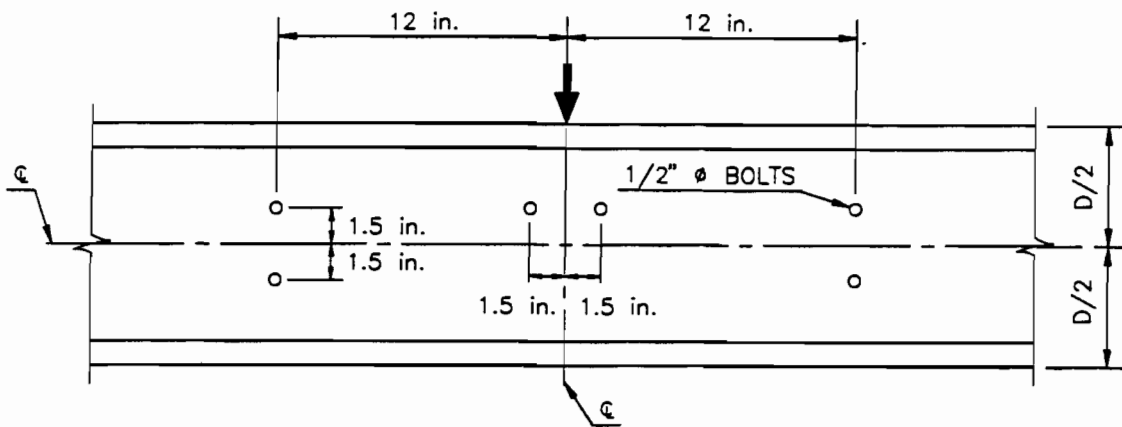
The I-beam specimens were fabricated by connecting two channel sections back-to-back with  $1/2$  inch diameter A325T bolts. This IOF study addressed the effect of different bolt configurations used to inter-connect the C-sections. The bolt patterns used in this study are shown in Figures 19a, 19b and 19c.

Before the specimens were connected together, small cold-formed steel channels were attached and served as transverse web stiffeners. For the case of the IOF loading condition, the portion of the web directly above the end supports was stiffened to force the failure to occur directly under the applied interior concentrated load. The stiffener locations are shown in Figure 14.

The fasteners used for restraining the flanges were two  $1/2$  inch diameter A325T bolts. For the IOF loading condition of I-sections, both flanges of the specimen below the interior concentrated load were fastened to the support as shown in Figure 20. For all I-beams tested, a  $5-1/4$  inch bearing length was used under the interior concentrated load and at the end supports. See Figures 21, 22 and 23 for the test specimen fabrication for the unfastened and the fastened flange I-beams subjected to the IOF loading condition.

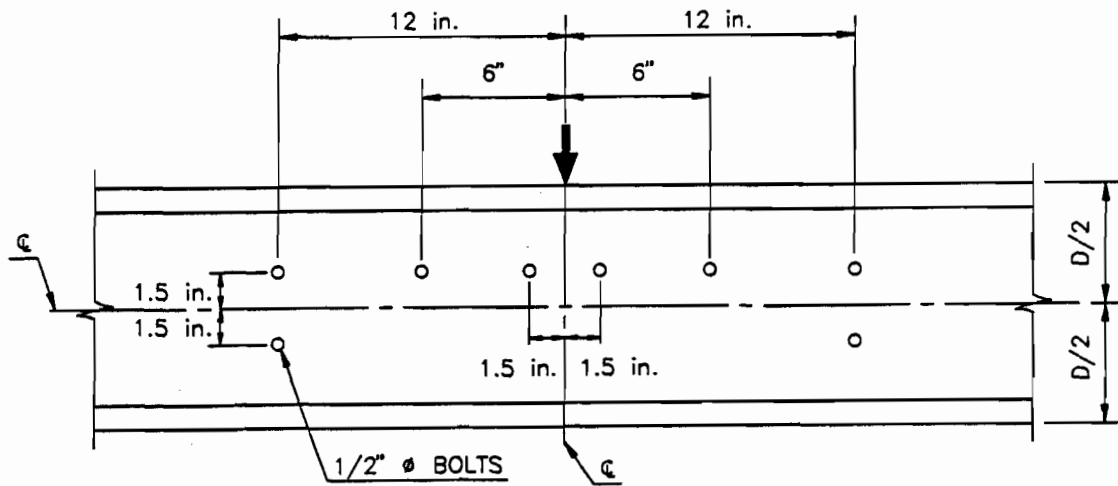


(a) Bolt Pattern One



(b) Bolt Pattern Two

Figure 19. Typical Bolt Patterns for I-Beams



(c) Bolt Pattern Three

Figure 19 (Cont'd.). Typical Bolt Patterns for I-Beams

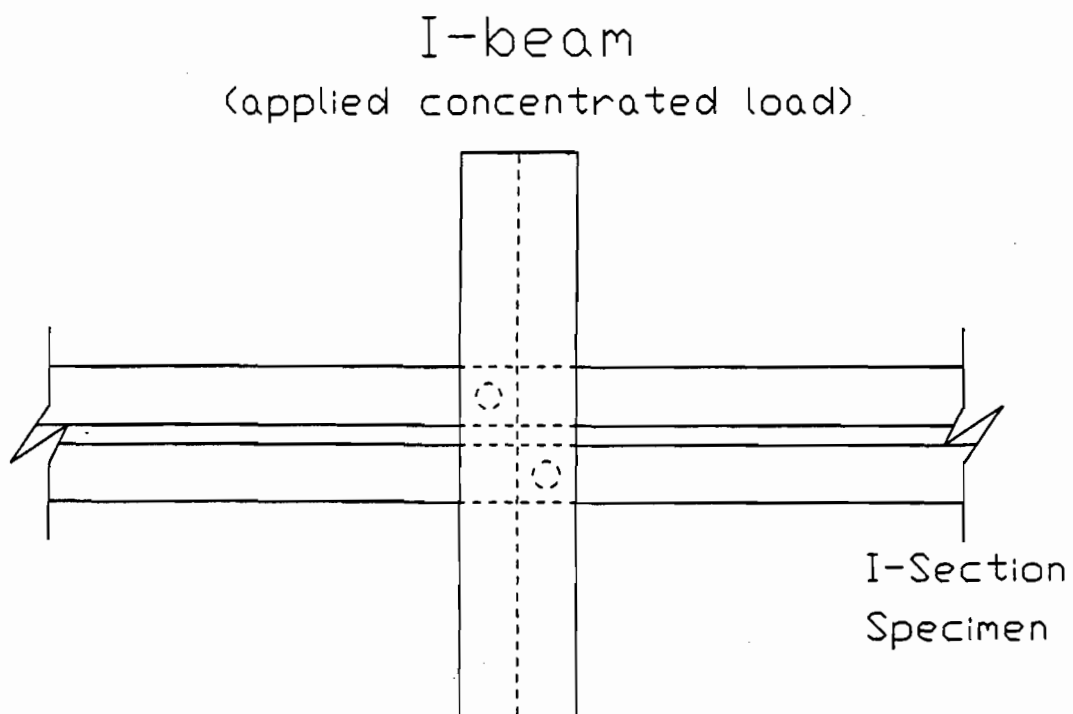


Figure 20. Top View of Typical Connection of an I-Beam with Flanges Restrained [6]

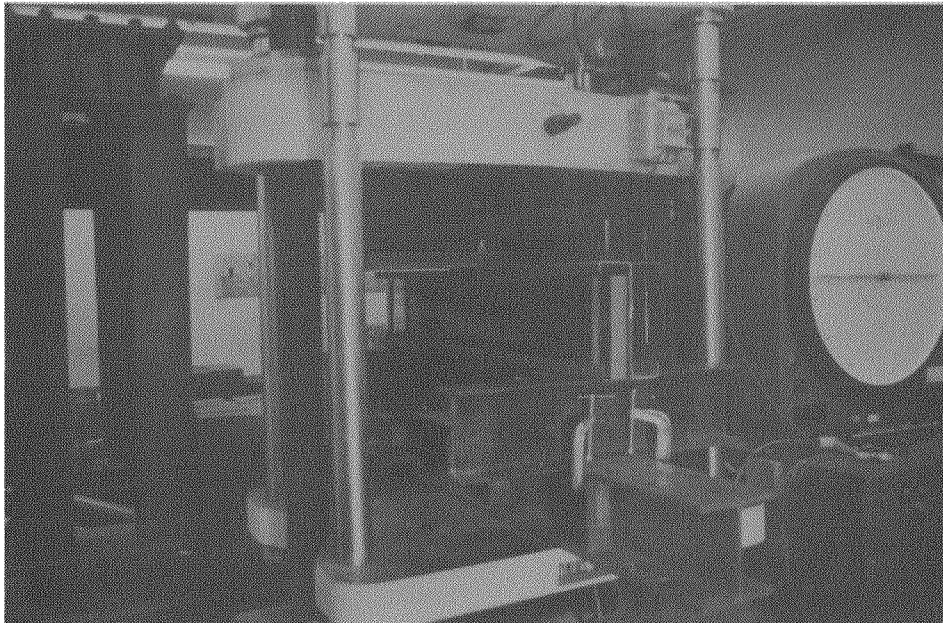


Figure 21. Photograph of Typical I-Beam Subjected to IOF Loading Condition with Restrained Flanges with Bolt Pattern One

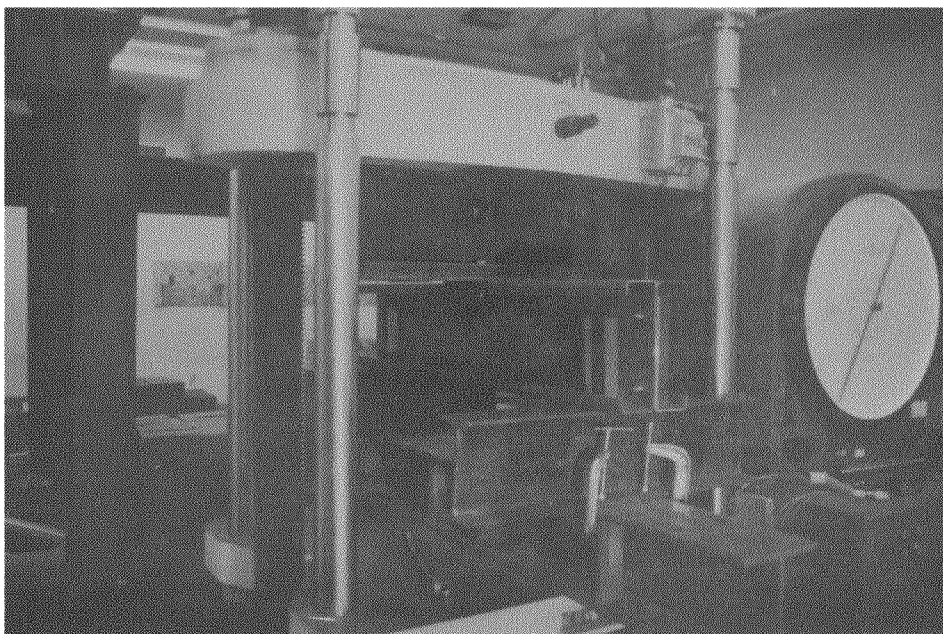
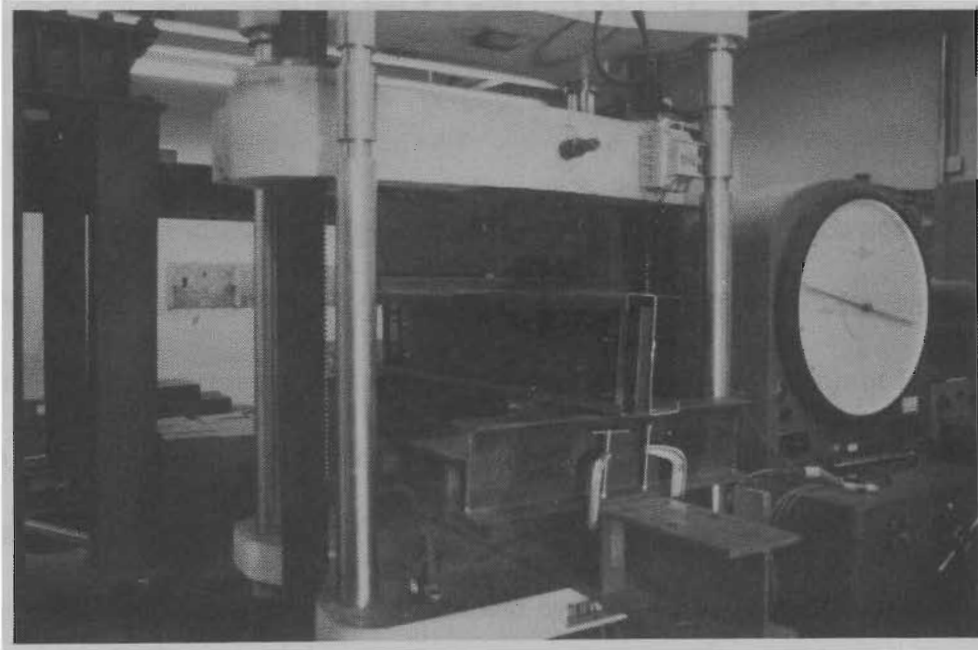


Figure 22. Photograph of a Typical I-Beam Subjected to IOF Loading Condition with Restrained Flanges with Bolt Pattern Two



**Figure 23. Photograph of a Typical I-Beam Subjected to IOF Loading Condition with Restrained Flanges with Bolt Pattern Three**



#### IV. TEST RESULTS AND EVALUATION OF DATA

##### A. GENERAL

The experimental data generated in this study is summarized and discussed in the following discussion. All test specimens were loaded to failure. The failure load values for identical specimens tested were very consistent. The total failure load obtained for each test specimen was divided by the number of webs responsible for carrying the applied concentrated load. The tested failure load per web is denoted by  $P_t$ . The computed load values per web are denoted by  $P_c$ .

##### B. TEST RESULTS

The evaluation of the experimental data is presented in tabular form for both the Z-sections and I-sections tested. The computed values were obtained by using the AISI Specification equations [3], the Prabakaran and Schuster equations [7], and the Santaputra, Parks and Yu equations [8]. Here after the above mentioned equations will be referred to as the AISI equation, the Prabakaran equation, and the Santaputra equation, respectively.

1. Z-Sections: A total of 28 Z-section specimens were tested for the EOF loading condition. One half of these specimens were tested with the flanges fastened to the supports, and the other half were tested with the flanges unfastened or unrestrained to the supports. Equations 8, 17, 18 and 19 were used to compute the web crippling loads of the Z-sections specimens. Tables V and VII show the cross-sectional dimensions

and equation parameters used in the computations of the Z-section's web crippling capacity. The results of the Z-sections tested are located in Tables IX through XX.

The Z1 specimens were the first to be tested, and have an  $h/t$  ratio of approximately 96. A measure of the accuracy of the prediction equations is the ratio  $P_t/P_c$ . As shown in Table IX, the unfastened flange specimens, Z1.1 and Z1.2, yielded good correlation to the AISI equation as demonstrated by the  $P_t/P_c$  ratios of 1.001 and 0.958. The Prabakaran equation overestimated the tested load by approximately 40 percent as shown by the  $P_t/P_c$  ratios of 0.610 and 0.584, respectively (Table X). The Santaputra equation, with  $P_t/P_c$  ratios of 0.933 and 0.894 (Table XI), gave unconservative correlation between the failure load and the computed load. The fastened flange specimens, Z1.3-F and Z1.4-F, yielded approximately 52 percent greater tested results than the AISI equation predicted based on the  $P_t/P_c$  ratios of 1.521 and 1.515, respectively. The Prabakaran equation yielded a conservative estimate of the tested failure load, as shown by  $P_t/P_c$  values of 0.927 and 0.923, respectively. The Santaputra equation underestimated the tested failure load by approximately 41 percent based on the  $P_t/P_c$  ratios of 1.419 and 1.414, respectively. The test results indicated an average 55.1 percent increase in strength between the fastened and the unfastened flange specimens as indicated by the  $P_f/P_{uf}$  ratio, where  $P_f$  represents the tested failure load with the specimen's flanges fastened to the supports and  $P_{uf}$  represents the tested failure load with the specimen's flanges unfastened to the supports.

The Z2 specimens had an  $h/t$  ratio of approximately 70. A measure of the accuracy of the prediction equations is the ratio  $P_t/P_c$ . As shown in Table IX, the unfastened flange specimens, Z2.1 and Z2.2, yielded approximately 16 percent less than

**Table IX. SUMMARY OF ALL Z-SECTION PARAMETERS, TEST LOADS, AND AISI COMPUTED LOADS**

Specimen No.	t (in.)	h (in.)	h/t	R/t	N/t	N/h	Fy (ksi)	Pt (kips)	Pf/Puf (Avg.)	AISI Equation	
										Pc (kips)	Pt/Pc
Z1.1	0.061	5.847	95.852	4.098	43.033	0.449	61.750	1.036		1.035	1.001
Z1.2	0.061	5.831	95.590	4.098	43.033	0.450	61.750	0.993		1.036	0.958
Z1.3-F	0.061	5.847	95.852	4.098	43.033	0.449	61.750	1.575		1.035	1.521
Z1.4-F	0.061	5.831	95.590	4.098	43.033	0.450	61.750	1.570	1.551	1.036	1.515
Z2.1	0.083	5.803	69.916	3.012	31.627	0.452	65.190	2.056		2.446	0.841
Z2.2	0.083	5.803	69.916	3.012	31.627	0.452	65.190	2.036		2.446	0.832
Z2.3-F	0.083	5.803	69.916	3.012	31.627	0.452	65.190	3.099		2.446	1.267
Z2.4-F	0.083	5.803	69.916	3.012	31.627	0.452	65.190	3.093	1.513	2.446	1.264

F = Represents specimens having flanges fastened to supports.

Pt = Test load per web.

Pc = Computed load per web.

Pf = Test load with flanges fastened to supports.

Puf = Test load with flanges unfastened to supports.

**Table X. SUMMARY OF ALL Z-SECTION PARAMETERS, TEST LOADS, AND PRABAKARAN COMPUTED LOADS**

Specimen No.	t (in.)	h (in.)	h/t	R/t	N/t	N/h	Fy (ksi)	Pt (kips)	Pf/Puf (Avg.)	Prabakaran Equation	
										Pc (kips)	Pt/Pc
Z1.1	0.061	5.847	95.852	4.098	43.033	0.449	61.750	1.036		1.699	0.610
Z1.2	0.061	5.831	95.590	4.098	43.033	0.450	61.750	0.993		1.701	0.584
Z1.3-F	0.061	5.847	95.852	4.098	43.033	0.449	61.750	1.575		1.699	0.927
Z1.4-F	0.061	5.831	95.590	4.098	43.033	0.450	61.750	1.570	1.551	1.701	0.923
Z2.1	0.083	5.803	69.916	3.012	31.627	0.452	65.190	2.056		3.554	0.579
Z2.2	0.083	5.803	69.916	3.012	31.627	0.452	65.190	2.036		3.554	0.573
Z2.3-F	0.083	5.803	69.916	3.012	31.627	0.452	65.190	3.099		3.554	0.872
Z2.4-F	0.083	5.803	69.916	3.012	31.627	0.452	65.190	3.093	1.513	3.554	0.870

F = Represents specimens having flanges fastened to supports.

Pt = Test load per web.

Pc = Computed load per web.

Pf = Test load with flanges fastened to supports.

Puf = Test load with flanges unfastened to supports.

**Table XI. SUMMARY OF ALL Z-SECTION PARAMETERS, TEST LOADS, AND SANTAPUTRA COMPUTED LOADS**

Specimen No.	t (in.)	h (in.)	h/t	R/t	N/t	N/h	Fy (ksi)	Pt (kips)	Pf/Puf (Avg.)	Santaputra Equation	
										Pc (kips)	Pt/Pc
Z1.1	0.061	5.847	95.852	4.098	43.033	0.449	61.750	1.036		1.110	0.933
Z1.2	0.061	5.831	95.590	4.098	43.033	0.450	61.750	0.993		1.110	0.894
Z1.3-F	0.061	5.847	95.852	4.098	43.033	0.449	61.750	1.575		1.110	1.419
Z1.4-F	0.061	5.831	95.590	4.098	43.033	0.450	61.750	1.570	1.551	1.110	1.414
Z2.1	0.083	5.803	69.916	3.012	31.627	0.452	65.190	2.056		1.972	1.043
Z2.2	0.083	5.803	69.916	3.012	31.627	0.452	65.190	2.036		1.972	1.033
Z2.3-F	0.083	5.803	69.916	3.012	31.627	0.452	65.190	3.099		1.972	1.572
Z2.4-F	0.083	5.803	69.916	3.012	31.627	0.452	65.190	3.093	1.513	1.972	1.568

F = Represents specimens having flanges fastened to supports.

Pt = Test load per web.

Pc = Computed load per web.

Pf = Test load with flanges fastened to supports.

Puf = Test load with flanges unfastened to supports.

**Table XII. SUMMARY OF ALL Z-SECTION PARAMETERS, TEST LOADS,  
AND AISI COMPUTED LOADS**

Specimen No.	t (in.)	h (in.)	h/t	R/t	N/t	N/h	Fy (ksi)	Pt (kips)	Pf/Puf (Avg.)	AISI Equation	
										Pc (kips)	Pt/Pc
Z3.1	0.061	7.847	128.639	4.098	43.033	0.335	62.030	1.261		0.960	1.314
Z3.2	0.061	7.862	128.885	4.098	43.033	0.334	62.030	1.205		0.959	1.256
Z3.3-F	0.061	7.847	128.639	4.098	43.033	0.335	62.030	1.703		0.960	1.773
Z3.4-F	0.061	7.862	128.885	4.098	43.033	0.334	62.030	1.745	1.399	0.959	1.819
Z4.1	0.083	7.818	94.193	3.012	31.627	0.336	63.050	1.955		2.315	0.844
Z4.2	0.083	7.818	94.193	3.012	31.627	0.336	63.050	2.011		2.315	0.869
Z4.3-F	0.083	7.834	94.386	3.012	31.627	0.335	63.050	2.766		2.314	1.195
Z4.4-F	0.083	7.834	94.386	3.012	31.627	0.335	63.050	2.725	1.385	2.314	1.177

F = Represents specimens having flanges fastened to supports.

Pt = Test load per web.

Pc = Computed load per web.

Pf = Test load with flanges fastened to supports.

Puf = Test load with flanges unfastened to supports.

**Table XIII. SUMMARY OF ALL Z-SECTION PARAMETERS, TEST LOADS, AND PRABAKARAN COMPUTED LOADS**

Specimen No.	t (in.)	h (in.)	h/t	R/t	N/t	N/h	Fy (ksi)	Pt (kips)	Pf/Puf (Avg.)	Prabakaran Equation	
										Pc (kips)	Pt/Pc
Z3.1	0.061	7.847	128.639	4.098	43.033	0.335	62.030	1.261		1.566	0.805
Z3.2	0.061	7.862	128.885	4.098	43.033	0.334	62.030	1.205		1.565	0.770
Z3.3-F	0.061	7.847	128.639	4.098	43.033	0.335	62.030	1.703		1.566	1.087
Z3.4-F	0.061	7.862	128.885	4.098	43.033	0.334	62.030	1.745	1.399	1.565	1.115
Z4.1	0.083	7.818	94.193	3.012	31.627	0.336	63.050	1.955		3.209	0.609
Z4.2	0.083	7.818	94.193	3.012	31.627	0.336	63.050	2.011		3.209	0.627
Z4.3-F	0.083	7.834	94.386	3.012	31.627	0.335	63.050	2.766		3.207	0.862
Z4.4-F	0.083	7.834	94.386	3.012	31.627	0.335	63.050	2.725	1.385	3.207	0.850

**F = Represents specimens having flanges fastened to supports.**

**Pt = Test load per web.**

**Pc = Computed load per web.**

**Pf = Test load with flanges fastened to supports.**

**Puf = Test load with flanges unfastened to supports.**

**Table XIV. SUMMARY OF ALL Z-SECTION PARAMETERS, TEST LOADS, AND SANTAPUTRA COMPUTED LOADS**

Specimen No.	t (in.)	h (in.)	h/t	R/t	N/t	N/h	Fy (ksi)	Pt (kips)	Pf/Puf (Avg.)	Santaputra Equation	
										Pc (kips)	Pt/Pc
Z3.1	0.061	7.847	128.639	4.098	43.033	0.335	62.030	1.261		1.115	1.131
Z3.2	0.061	7.862	128.885	4.098	43.033	0.334	62.030	1.205		1.115	1.081
Z3.3-F	0.061	7.847	128.639	4.098	43.033	0.335	62.030	1.703		1.115	1.527
Z3.4-F	0.061	7.862	128.885	4.098	43.033	0.334	62.030	1.745	1.399	1.115	1.565
Z4.1	0.083	7.818	94.193	3.012	31.627	0.336	63.050	1.955		1.907	1.025
Z4.2	0.083	7.818	94.193	3.012	31.627	0.336	63.050	2.011		1.907	1.055
Z4.3-F	0.083	7.834	94.386	3.012	31.627	0.335	63.050	2.766		1.907	1.451
Z4.4-F	0.083	7.834	94.386	3.012	31.627	0.335	63.050	2.725	1.385	1.907	1.429

F = Represents specimens having flanges fastened to supports.

Pt = Test load per web.

Pc = Computed load per web.

Pf = Test load with flanges fastened to supports.

Puf = Test load with flanges unfastened to supports.



**Table XV. SUMMARY OF ALL Z-SECTION PARAMETERS, TEST LOADS, AND AISI COMPUTED LOADS**

Specimen No.	t (in.)	h (in.)	h/t	R/t	N/t	N/h	Fy (ksi)	Pt (kips)	Pf/Puf (Avg.)	AISI Equation	
										Pc (kips)	Pt/Pc
Z5.1	0.059	8.882	150.542	4.237	44.492	0.296	73.110	1.048		0.821	1.275
Z5.2	0.059	8.866	150.271	4.237	44.492	0.296	73.110	1.055		0.822	1.284
Z5.3-F	0.059	8.882	150.542	4.237	44.492	0.296	73.110	1.391		0.821	1.694
Z5.4-F	0.059	8.866	150.271	4.237	44.492	0.296	73.110	1.473	1.362	0.822	1.792
Z6.1	0.075	8.834	117.787	3.333	35.000	0.297	73.780	1.860		1.694	1.098
Z6.2	0.075	8.85	118.000	3.333	35.000	0.297	73.780	1.895		1.693	1.119
Z6.3-F	0.075	8.834	117.787	3.333	35.000	0.297	73.780	2.469		1.694	1.457
Z6.4-F	0.075	8.85	118.000	3.333	35.000	0.297	73.780	2.518	1.328	1.693	1.487

**F = Represents specimens having flanges fastened to supports.**

**Pt = Test load per web.**

**Pc = Computed load per web.**

**Pf = Test load with flanges fastened to supports.**

**Puf = Test load with flanges unfastened to supports.**

**Table XVI. SUMMARY OF ALL Z-SECTION PARAMETERS, TEST LOADS, AND PRABAKARAN COMPUTED LOADS**

Specimen No.	t (in.)	h (in.)	h/t	R/t	N/t	N/h	Fy (ksi)	Pt (kips)	Pf/Puf (Avg.)	Prabakaran Equation	
										Pc (kips)	Pt/Pc
Z5.1	0.059	8.882	150.542	4.237	44.492	0.296	73.110	1.048		1.632	0.642
Z5.2	0.059	8.866	150.271	4.237	44.492	0.296	73.110	1.055		1.633	0.646
Z5.3-F	0.059	8.882	150.542	4.237	44.492	0.296	73.110	1.391		1.632	0.853
Z5.4-F	0.059	8.866	150.271	4.237	44.492	0.296	73.110	1.473	1.362	1.633	0.902
Z6.1	0.075	8.834	117.787	3.333	35.000	0.297	73.780	1.860		2.894	0.643
Z6.2	0.075	8.85	118.000	3.333	35.000	0.297	73.780	1.895		2.892	0.655
Z6.3-F	0.075	8.834	117.787	3.333	35.000	0.297	73.780	2.469		2.894	0.853
Z6.4-F	0.075	8.85	118.000	3.333	35.000	0.297	73.780	2.518	1.328	2.892	0.871

F = Represents specimens having flanges fastened to supports.

Pt = Test load per web.

Pc = Computed load per web.

Pf = Test load with flanges fastened to supports.

Puf = Test load with flanges unfastened to supports.

**Table XVII. SUMMARY OF ALL Z-SECTION PARAMETERS, TEST LOADS,  
AND SANTAPUTRA COMPUTED LOADS**

Specimen No.	t (in.)	h (in.)	h/t	R/t	N/t	N/h	Fy (ksi)	Pt (kips)	Pf/Puf (Avg.)	Santaputra Equation	
										Pc (kips)	Pt/Pc
Z5.1	0.059	8.882	150.542	4.237	44.492	0.296	73.110	1.048		1.244	0.842
Z5.2	0.059	8.866	150.271	4.237	44.492	0.296	73.110	1.055		1.244	0.848
Z5.3-F	0.059	8.882	150.542	4.237	44.492	0.296	73.110	1.391		1.244	1.118
Z5.4-F	0.059	8.866	150.271	4.237	44.492	0.296	73.110	1.473	1.362	1.244	1.184
Z6.1	0.075	8.834	117.787	3.333	35.000	0.297	73.780	1.860		1.876	0.991
Z6.2	0.075	8.85	118.000	3.333	35.000	0.297	73.780	1.895		1.876	1.010
Z6.3-F	0.075	8.834	117.787	3.333	35.000	0.297	73.780	2.469		1.876	1.316
Z6.4-F	0.075	8.85	118.000	3.333	35.000	0.297	73.780	2.518	1.328	1.876	1.342

**F = Represents specimens having flanges fastened to supports.**

**Pt = Test load per web.**

**Pc = Computed load per web.**

**Pf = Test load with flanges fastened to supports.**

**Puf = Test load with flanges unfastened to supports.**

**Table XVIII. SUMMARY OF ALL Z-SECTION PARAMETERS, TEST LOADS,  
AND AISI COMPUTED LOADS**

Specimen No.	t (in.)	h (in.)	h/t	R/t	N/t	N/h	Fy (ksi)	Pt (kips)	Pf/Puf (Avg.)	AISI Equation	
										Pc (kips)	Pt/Pc
Z7.1	0.075	10.74	143.200	4.173	35.000	0.244	56.890	1.524		1.272	1.197
Z7.2	0.075	10.724	142.987	4.173	35.000	0.245	56.890	1.529		1.273	1.201
Z7.3-F	0.075	10.74	143.200	4.173	35.000	0.244	56.890	2.024		1.272	1.590
Z7.4-F	0.075	10.724	142.987	4.173	35.000	0.245	56.890	2.050	1.335	1.273	1.610

**F = Represents specimens having flanges fastened to supports.**

**Pt = Test load per web.**

**Pc = Computed load per web.**

**Pf = Test load with flanges fastened to supports.**

**Puf = Test load with flanges unfastened to supports.**

**Table XIX. SUMMARY OF ALL Z-SECTION PARAMETERS, TEST LOADS, AND PRABAKARAN COMPUTED LOADS**

Specimen No.	t (in.)	h (in.)	h/t	R/t	N/t	N/h	Fy (ksi)	Pt (kips)	Pf/Puf (Avg.)	Prabakaran Equation	
										Pc (kips)	Pt/Pc
Z7.1	0.075	10.74	143.200	4.173	35.000	0.244	56.890	1.524		1.911	0.797
Z7.2	0.075	10.724	142.987	4.173	35.000	0.245	56.890	1.529		1.912	0.800
Z7.3-F	0.075	10.74	143.200	4.173	35.000	0.244	56.890	2.024		1.911	1.059
Z7.4-F	0.075	10.724	142.987	4.173	35.000	0.245	56.890	2.050	1.335	1.912	1.072

F = Represents specimens having flanges fastened to supports.

Pt = Test load per web.

Pc = Computed load per web.

Pf = Test load with flanges fastened to supports.

Puf = Test load with flanges unfastened to supports.

**Table XX. SUMMARY OF ALL Z-SECTION PARAMETERS, TEST LOADS, AND SANTAPUTRA COMPUTED LOADS**

Specimen No.	t (in.)	h (in.)	h/t	R/t	N/t	N/h	Fy (ksi)	Pt (kips)	Pf/Puf (Avg.)	Santaputra Equation	
										Pc (kips)	Pt/Pc
Z7.1	0.075	10.74	143.200	4.173	35.000	0.244	56.890	1.524		1.447	1.053
Z7.2	0.075	10.724	142.987	4.173	35.000	0.245	56.890	1.529		1.447	1.057
Z7.3-F	0.075	10.74	143.200	4.173	35.000	0.244	56.890	2.024		1.447	1.399
Z7.4-F	0.075	10.724	142.987	4.173	35.000	0.245	56.890	2.050	1.335	1.447	1.417

F = Represents specimens having flanges fastened to supports.

Pt = Test load per web.

Pc = Computed load per web.

Pf = Test load with flanges fastened to supports.

Puf = Test load with flanges unfastened to supports.

the AISI equation predicted as demonstrated by the  $P_t/P_c$  ratios of 0.841 and 0.832. The Prabakaran equation overestimated the tested load by approximately 42 percent as indicated by the  $P_t/P_c$  ratios of 0.579 and 0.573, respectively (Table X). The Santaputra equation, with  $P_t/P_c$  ratios of 1.043 and 1.033 (Table XI), gave slightly conservative correlation between the failure load and the computed load. The fastened flange specimens, Z2.3-F and Z2.4-F, developed approximately 26 percent greater tested load capacity than the AISI equation predicted based on the  $P_t/P_c$  ratios of 1.267 and 1.264, respectively. The Prabakaran equation provided a conservative estimate of the tested failure load, as shown by  $P_t/P_c$  values of 0.872 and 0.870, respectively. The Santaputra equation underestimated the tested failure load by approximately 57 percent as indicated by the  $P_t/P_c$  ratios of 1.572 and 1.568, respectively. The test results indicated an average 51.3 percent increase in strength between the fastened and the unfastened flange specimens as indicated by the  $P_f/P_{uf}$  ratio, where  $P_f$  represents the tested failure load with the specimens flanges fastened to the supports and  $P_{uf}$  represents the tested failure load with the specimens flanges unfastened to the supports.

The Z3 specimens had an  $h/t$  ratio of approximately 129. A measure of the accuracy of the prediction equations is the ratio  $P_t/P_c$ . As shown in Table XII, the unfastened flange specimens, Z3.1 and Z3.2, yielded approximately 28 percent more test load capacity than the AISI equation predicted as demonstrated by the  $P_t/P_c$  ratios of 1.314 and 1.256, respectively. The Prabakaran equation overestimated the tested load by approximately 21 percent as seen by the  $P_t/P_c$  ratios of 0.805 and 0.770, respectively (Table XIII). The Santaputra equation, with  $P_t/P_c$  ratios of 1.131 and 1.081 (Table XIV), gave conservative correlation between the failure load and the computed load. The

fastened flange specimens, Z3.3-F and Z3.4-F, yielded approximately 79 percent greater tested results than the AISI equation predicted based on the  $P_t/P_c$  ratios of 1.773 and 1.819, respectively. The Prabakaran equation yielded a conservative estimate of the tested failure load, as shown by  $P_t/P_c$  values of 1.087 and 1.115, respectively. The Santaputra equation underestimated the tested failure load by approximately 54 percent based on the  $P_t/P_c$  ratios of 1.527 and 1.565, respectively. The test results indicated an average 39.9 percent increase in strength between the fastened and the unfastened flange specimens as indicated by the  $P_t/P_{uf}$  ratio, where  $P_t$  represents the tested failure load with the specimen's flanges fastened to the supports and  $P_{uf}$  represents the tested failure load with the specimen's flanges unfastened.

The Z4 specimens had an  $h/t$  ratio of approximately 94. A measure of the accuracy of the prediction equations is the ratio  $P_t/P_c$ . As shown in Table XII, the unfastened flange specimens, Z4.1 and Z4.2, yielded approximately 15 percent less load capacity than the AISI equation predicted as demonstrated by the  $P_t/P_c$  ratios of 0.844 and 0.869, respectively. The Prabakaran equation overestimated the tested load by approximately 38 percent based on the  $P_t/P_c$  ratios of 0.609 and 0.627, respectively (Table XIII). The Santaputra equation, with  $P_t/P_c$  ratios of 1.025 and 1.055 (Table XIV), gave slightly conservative correlation between the tested failure load and the computed load. The fastened flange specimens, Z4.3-F and Z4.4-F, yielded approximately 18 percent greater tested results than the AISI equation predicted as seen by the  $P_t/P_c$  ratios of 1.195 and 1.177, respectively. The Prabakaran equation yielded a conservative estimate of the tested failure load, as shown by  $P_t/P_c$  values of 0.862 and 0.850, respectively. The Santaputra equation underestimated the tested failure load by nearly



44 percent as seen by the  $P_t/P_c$  ratios of 1.451 and 1.429, respectively. The test results indicated an average 38.5 percent increase in strength between the fastened and the unfastened flange specimens as indicated by the  $P_f/P_{uf}$  ratio, where  $P_f$  represents the tested failure load with the specimen's flanges fastened to the supports and  $P_{uf}$  represents the tested failure load with the specimen's flanges unfastened.

The Z5 specimens had an  $h/t$  ratio of approximately 150. A measure of the accuracy of the prediction equations is the ratio  $P_t/P_c$ . As shown in Table XV, the unfastened flange specimens, Z5.1 and Z5.2, yielded approximately 28 percent more web capacity than the AISI equation predicted, as demonstrated by the  $P_t/P_c$  ratios of 1.275 and 1.284, respectively. The Prabakaran equation overestimated the tested load by approximately 35 percent based on the  $P_t/P_c$  ratios of 0.642 and 0.646, respectively (Table XVI). The Santaputra equation, with  $P_t/P_c$  ratios of 0.842 and 0.848 (Table XVII), gave unconservative correlation between the failure load and the computed load. The fastened flange specimens, Z5.3-F and Z5.4-F, yielded approximately 74 percent greater tested results than the AISI equation predicted as seen by the  $P_t/P_c$  ratios of 1.694 and 1.792, respectively. The Prabakaran equation yielded a conservative estimate of the tested failure load, as shown by  $P_t/P_c$  values of 0.853 and 0.902, respectively. The Santaputra equation underestimated the tested failure load by approximately 15 percent as seen by the  $P_t/P_c$  ratios of 1.118 and 1.184, respectively. The test results indicated an average 36.2 percent increase in strength between the fastened and the unfastened flange specimens as indicated by the  $P_f/P_{uf}$  ratio, where  $P_f$  represents the tested failure load with the specimens flanges fastened to the supports and  $P_{uf}$  represents the tested failure load with the specimens flanges unfastened to the supports.

The Z6 specimens had an  $h/t$  ratio of approximately 118. A measure of the accuracy of the prediction equations is the ratio  $P_t/P_c$ . As shown in Table XV, the unfastened flange specimens, Z6.1 and Z6.2, yielded approximately 10 percent more web capacity than the AISI equation predicted as demonstrated by the  $P_t/P_c$  ratios of 1.098 and 1.119, respectively. The Prabakaran equation overestimated the tested load by approximately 35 percent as seen by the  $P_t/P_c$  ratios of 0.643 and 0.655, respectively (Table XVI). The Santaputra equation, with  $P_t/P_c$  ratios of 0.991 and 1.010 (Table XVII), gave unconservative correlation between the failure load and the computed load. The fastened flange specimens, Z6.3-F and Z6.4-F, yielded approximately 47 percent greater tested load capacity results than the AISI equation predicted as given by the  $P_t/P_c$  ratios of 1.457 and 1.487, respectively. The Prabakaran equation yielded an unconservative estimate of the tested failure load, as shown by  $P_t/P_c$  values of 0.853 and 0.871, respectively. The Santaputra equation underestimated the tested failure load by approximately 33 percent due to the  $P_t/P_c$  ratios of 1.316 and 1.342, respectively. The test results indicated an average 32.8 percent increase in strength between the fastened and the unfastened flange specimens as indicated by the  $P_f/P_{uf}$  ratio, where  $P_f$  represents the tested failure load with the specimens flanges fastened to the supports and  $P_{uf}$  represents the tested failure load with the specimens flanges unfastened to the supports.

The Z7 specimens had an  $h/t$  ratio of approximately 143. A measure of the accuracy of the prediction equations is the ratio  $P_t/P_c$ . As shown in Table XVIII, the unfastened flange specimens, Z7.1 and Z7.2, yielded approximately 20 percent more web strength than the AISI equation predicted as demonstrated by the  $P_t/P_c$  ratios of 1.197 and 1.201, respectively. The Prabakaran equation overestimated the tested load by nearly

20 percent as given by the  $P_f/P_c$  ratios of 0.797 and 0.800, respectively (Table XIX). The Santaputra equation, with  $P_f/P_c$  ratios of 1.053 and 1.057 (Table XX), gave conservative correlation between the failure load and the computed load. The fastened flange specimens, Z7.3-F and Z7.4-F, yielded approximately 60 percent greater tested load capacity results than the AISI equation predicted based on the  $P_f/P_c$  ratios of 1.590 and 1.610, respectively. The Prabakaran equation yielded a conservative estimate of the tested failure load, as shown by  $P_f/P_c$  values of 1.059 and 1.072, respectively. The Santaputra equation underestimated the tested failure load by approximately 40 percent as seen by the  $P_f/P_c$  ratios of 1.399 and 1.417, respectively. The test results indicated an average 33.5 percent increase in strength between the fastened and the unfastened flange specimens as indicated by the  $P_f/P_{uf}$  ratio, where  $P_f$  represents the tested failure load with the specimens flanges fastened to the supports and  $P_{uf}$  represents the tested failure load with the specimens flanges unfastened to the supports.

The failure modes that were observed during this investigation were recorded by taking photographs of the specimens under loading. Photographs of typical failure modes of the unfastened flange and fastened flange specimens are shown in Figures 15 through 18. The failure modes that resulted from the EOF loading condition without the flanges fastened to the support was a combination of vertical deflection of the bottom flanges, commonly called flange curling, and reverse curvature in the webs was observed directly above the end supports. The test specimens that had restrained flanges were limited to only reverse curvature in the webs and no flange curling occurred, therefore allowing the specimen to reach a higher failure load.

2. I-Sections: A total of 14 I-section specimens were tested by being subjected to an IOF loading condition. Twelve of which were tested with the flanges fastened to the supports, and two were tested with the flanges unfastened. Equations 12, 17, 20 and 21 were used to compute the web crippling loads for the I-section test specimens. Tables VI and VIII show the cross-section dimensions and equation parameters used in the computations of the I-sections. The results of the I-sections tested are located in Tables XXI through XXVIII.

The objective of these I-section tests was to identify if there is any significant increase in web crippling strength when different bolt configurations are used to inter-connect the webs of two channel sections forming an I-section. A secondary objective was to assess the appropriate uses of the AISI multiple web crippling equation and the AISI single web crippling equation.

The I-sections I1 and I1-F through I6-F had an  $h/t$  ratio of approximately 112. A measure of the accuracy of the prediction equations is the ratio  $P_t/P_c$ . The I1, I1-F and the I2-F specimens were inter-connected using bolt pattern one (Figure 19a). The I3-F and the I4-F specimens were inter-connected by using bolt pattern two as shown in Figure 19b. The I5-F and I6-F specimens were inter-connected by using bolt pattern three as shown in Figure 19c. As shown in Table XXI, the unfastened flange specimen, I1, yielded no substantial difference between the tested failure load and the AISI multiple web equation failure load as demonstrated by the  $P_t/P_c$  ratio of 0.832. The AISI single web equation underestimated the tested failure load by approximately 20 percent because  $P_t/P_c$  ratio was 1.202 (Table XXII). The Prabakaran equation overestimated the failure

**Table XXI. SUMMARY OF ALL I-SECTION PARAMETERS, TEST LOADS, AND AISI MULTIPLE WEB EQUATION COMPUTED LOADS**

Specimen No.	t (in.)	h (in.)	h/t	R/t	N/t	N/h	Fy (ksi)	Pt (kips)	AISI Equation		
									Pc (kips)	Pt/Pc	Pt/Pc (Avg.)
I1	0.067	7.507	112.045	2.328	78.358	0.699	61.200	5.935	7.137	0.832	
I1-F	0.067	7.507	112.045	2.328	78.358	0.699	61.200	6.048	7.137	0.847	
I2-F	0.067	7.475	111.567	2.328	78.358	0.702	61.200	6.010	7.137	0.842	
I3-F	0.067	7.492	111.821	2.328	78.358	0.701	61.200	6.223	7.137	0.872	
I4-F	0.067	7.475	111.567	2.328	78.358	0.702	61.200	6.060	7.137	0.849	
I5-F	0.067	7.492	111.821	2.328	78.358	0.701	61.200	6.173	7.137	0.865	
I6-F	0.067	7.507	112.045	2.328	78.358	0.699	61.200	6.285	7.137	0.881	0.855

**F = Represents flanges fastened to supports.**

**Pt = Test load per web.**

**Pc = Computed load per web.**

**Table XXII. SUMMARY OF ALL I-SECTION PARAMETERS, TEST LOADS, AND AISI SINGLE WEB EQUATION COMPUTED LOADS**

Specimen No.	t (in.)	h (in.)	h/t	R/t	N/t	N/h	Fy (ksi)	Pt (kips)	AISI Equation		
									Pc (kips)	Pt/Pc	Pt/Pc (Avg.)
I1	0.067	7.507	112.045	2.328	78.358	0.699	61.200	5.935	4.938	1.202	
I1-F	0.067	7.507	112.045	2.328	78.358	0.699	61.200	6.048	4.938	1.225	
I2-F	0.067	7.475	111.567	2.328	78.358	0.702	61.200	6.010	4.941	1.216	
I3-F	0.067	7.492	111.821	2.328	78.358	0.701	61.200	6.223	4.939	1.260	
I4-F	0.067	7.475	111.567	2.328	78.358	0.702	61.200	6.060	4.941	1.226	
I5-F	0.067	7.492	111.821	2.328	78.358	0.701	61.200	6.173	4.939	1.250	
I6-F	0.067	7.507	112.045	2.328	78.358	0.699	61.200	6.285	4.938	1.273	1.236

F = Represents flanges fastened to supports.

Pt = Test load per web.

Pc = Computed load per web.

**Table XXIII. SUMMARY OF ALL I-SECTION PARAMETERS, TEST LOADS, AND PRABAKARAN COMPUTED LOADS**

Specimen No.	t (in.)	h (in.)	h/t	R/t	N/t	N/h	Fy (ksi)	Pt (kips)	Prabakaran Equation		
									Pc (kips)	Pt/Pc	Pt/Pc (Avg.)
I1	0.067	7.507	112.045	2.328	78.358	0.699	61.200	5.935	8.129	0.730	
I1-F	0.067	7.507	112.045	2.328	78.358	0.699	61.200	6.048	8.129	0.744	
I2-F	0.067	7.475	111.567	2.328	78.358	0.702	61.200	6.010	8.129	0.739	
I3-F	0.067	7.492	111.821	2.328	78.358	0.701	61.200	6.223	8.129	0.765	
I4-F	0.067	7.475	111.567	2.328	78.358	0.702	61.200	6.060	8.129	0.745	
I5-F	0.067	7.492	111.821	2.328	78.358	0.701	61.200	6.173	8.129	0.759	
I6-F	0.067	7.507	112.045	2.328	78.358	0.699	61.200	6.285	8.129	0.773	0.751

F = Represents flanges fastened to supports.

Pt = Test load per web.

Pc = Computed load per web.

**Table XXIV. SUMMARY OF ALL I-SECTION PARAMETERS, TEST LOADS, AND SANTAPUTRA COMPUTED LOADS**

Specimen No.	t (in.)	h (in.)	h/t	R/t	N/t	N/h	Fy (ksi)	Pt (kips)	Pc (kips)	Santaputra Equation	
										Pt/Pc	Pt/Pc (Avg.)
I1	0.067	7.507	112.045	2.328	78.358	0.699	61.200	5.935	6.141	0.966	
I1-F	0.067	7.507	112.045	2.328	78.358	0.699	61.200	6.048	6.141	0.985	
I2-F	0.067	7.475	111.567	2.328	78.358	0.702	61.200	6.010	6.143	0.978	
I3-F	0.067	7.492	111.821	2.328	78.358	0.701	61.200	6.223	6.142	1.013	
I4-F	0.067	7.475	111.567	2.328	78.358	0.702	61.200	6.060	6.143	0.987	
I5-F	0.067	7.492	111.821	2.328	78.358	0.701	61.200	6.173	6.142	1.005	
I6-F	0.067	7.507	112.045	2.328	78.358	0.699	61.200	6.285	6.141	1.023	0.994

**F = Represents flanges fastened to supports.**

**Pt = Test load per web.**

**Pc = Computed load per web.**



**Table XXV. SUMMARY OF ALL I-SECTION PARAMETERS, TEST LOADS, AND AISI MULTIPLE WEB EQUATION COMPUTED LOADS**

Specimen No.	t (in.)	h (in.)	h/t	R/t	N/t	N/h	Fy (ksi)	Pt (kips)	AISI Equation		
									Pc (kips)	Pt/Pc	Pt/Pc (Avg.)
I7	0.085	7.581	89.188	1.835	61.765	0.693	63.340	9.788	11.332	0.864	
I7-F	0.085	7.581	89.188	1.835	61.765	0.693	63.340	10.285	11.332	0.908	
I8-F	0.085	7.518	88.447	1.835	61.765	0.698	63.340	10.060	11.332	0.888	
I9-F	0.085	7.502	88.259	1.835	61.765	0.700	63.340	9.998	11.332	0.882	
I10-F	0.085	7.518	88.447	1.835	61.765	0.698	63.340	9.985	11.332	0.881	
I11-F	0.085	7.502	88.259	1.835	61.765	0.700	63.340	10.610	11.332	0.936	
I12-F	0.085	7.581	89.188	1.835	61.765	0.693	63.340	10.285	11.332	0.908	0.895

F = Represents flanges fastened to supports.

Pt = Test load per web.

Pc = Computed load per web.

**Table XXVI. SUMMARY OF ALL I-SECTION PARAMETERS, TEST LOADS, AND AISI SINGLE WEB EQUATION COMPUTED LOADS**

Specimen No.	t (in.)	h (in.)	h/t	R/t	N/t	N/h	Fy (ksi)	Pt (kips)	AISI Equation		
									Pc (kips)	Pt/Pc	Pt/Pc (Avg.)
I7	0.085	7.581	89.188	1.835	61.765	0.693	63.340	9.788	7.670	1.276	
I7-F	0.085	7.581	89.188	1.835	61.765	0.693	63.340	10.285	7.670	1.341	
I8-F	0.085	7.518	88.447	1.835	61.765	0.698	63.340	10.060	7.679	1.310	
I9-F	0.085	7.502	88.259	1.835	61.765	0.700	63.340	9.998	7.681	1.302	
I10-F	0.085	7.518	88.447	1.835	61.765	0.698	63.340	9.985	7.679	1.300	
I11-F	0.085	7.502	88.259	1.835	61.765	0.700	63.340	10.610	7.681	1.381	
I12-F	0.085	7.581	89.188	1.835	61.765	0.693	63.340	10.285	7.670	1.341	1.322

F = Represents flanges fastened to supports.

Pt = Test load per web.

Pc = Computed load per web.

**Table XXVII. SUMMARY OF ALL I-SECTION PARAMETERS, TEST LOADS, AND PRABAKARAN COMPUTED LOADS**

Specimen No.	t (in.)	h (in.)	h/t	R/t	N/t	N/h	Fy (ksi)	Pt (kips)	Prabakaran Equation		
									Pc (kips)	Pt/Pc	Pt/Pc (Avg.)
I7	0.085	7.581	89.188	1.835	61.765	0.693	63.340	9.788	12.951	0.756	
I7-F	0.085	7.581	89.188	1.835	61.765	0.693	63.340	10.285	12.951	0.794	
I8-F	0.085	7.518	88.447	1.835	61.765	0.698	63.340	10.060	12.952	0.777	
I9-F	0.085	7.502	88.259	1.835	61.765	0.700	63.340	9.998	12.952	0.772	
I10-F	0.085	7.518	88.447	1.835	61.765	0.698	63.340	9.985	12.952	0.771	
I11-F	0.085	7.502	88.259	1.835	61.765	0.700	63.340	10.610	12.952	0.819	
I12-F	0.085	7.581	89.188	1.835	61.765	0.693	63.340	10.285	12.951	0.794	0.783

F = Represents flanges fastened to supports.

Pt = Test load per web.

Pc = Computed load per web.

**Table XXVIII. SUMMARY OF ALL I-SECTION PARAMETERS, TEST LOADS, AND SANTAPUTRA COMPUTED LOADS**

Specimen No.	t (in.)	h (in.)	h/t	R/t	N/t	N/h	Fy (ksi)	Pt (kips)	Pc (kips)	Santaputra Equation	
										Pt/Pc	Pt/Pc (Avg.)
I7	0.085	7.581	89.188	1.835	61.765	0.693	63.340	9.788	9.997	0.979	
I7-F	0.085	7.581	89.188	1.835	61.765	0.693	63.340	10.285	9.997	1.029	
I8-F	0.085	7.518	88.447	1.835	61.765	0.698	63.340	10.060	10.000	1.006	
I9-F	0.085	7.502	88.259	1.835	61.765	0.700	63.340	9.998	10.001	1.000	
I10-F	0.085	7.518	88.447	1.835	61.765	0.698	63.340	9.985	10.000	0.998	
I11-F	0.085	7.502	88.259	1.835	61.765	0.700	63.340	10.610	10.001	1.061	
I12-F	0.085	7.581	89.188	1.835	61.765	0.693	63.340	10.285	9.997	1.029	1.015

F = Represents flanges fastened to supports.

Pt = Test load per web.

Pc = Computed load per web.

load by approximately 27 percent as seen by the  $P_t/P_c$  ratio of 0.730 (Table XXIII). The Santaputra equation yielded a  $P_t/P_c$  ratio of 0.966 (Table XXIV) which gave reasonably good correlation between the failure and the computed load. The fastened flange specimens, I1-F through I6-F, yielded, on average, approximately 14 percent greater computed failure loads than the tested failure loads as calculated by the AISI multiple web equation and is shown by the average  $P_t/P_c$  ratio of 0.855 (Table XXI). The AISI single web equation underestimated the tested failure load by approximately 23 percent because the average  $P_t/P_c$  ratio was 1.236 (Table XXII). The Prabakaran equation overestimated the failure load by approximately 25 percent due to the average  $P_t/P_c$  ratio of 0.751 (Table XXIII). The Santaputra equation, with an average  $P_t/P_c$  ratio of 0.994 (Table XXIV), gave good correlation between the failure and the computed load. The range of values for  $P_t$  shows that the bolt patterns did not have a significant impact on the strength of the sections tested.

The I-sections I7 and I7-F through I12-F had an  $h/t$  ratio of approximately 89. A measure of the accuracy of the prediction equations is the ratio  $P_t/P_c$ . The I7, I7-F and the I8-F specimens were inter-connected using bolt pattern one (Figure 19a). The I9-F and the I10-F specimens were inter-connected by using bolt pattern two as shown in Figure 19b. The I11-F and I12-F specimens were inter-connected by using bolt pattern three as shown in Figure 19c. As shown in Table XXV, the unfastened flange specimen, I7, yielded no substantial difference between the tested failure load and the AISI multiple web equation failure load as demonstrated by the  $P_t/P_c$  ratio of 0.864. The AISI single web equation underestimated the tested failure load by approximately 28 percent because  $P_t/P_c$  ratio was 1.276 (Table XXVI). The Prabakaran equation overestimated the failure

load by approximately 24 percent as seen by the  $P_t/P_c$  ratio of 0.756 (Table XXVII). The Santaputra equation, with a  $P_t/P_c$  ratio of 0.979 (Table XXVIII), gave reasonably good correlation between the failure and the computed load. The fastened flange specimens, I7-F through I12-F, yielded, on average, approximately 11 percent greater computed failure loads than the tested failure loads as calculated by the AISI multiple web equation and is shown by the average  $P_t/P_c$  ratio of 0.895 (Table XXV). The AISI single web equation underestimated the tested failure load by approximately 32 percent because the average  $P_t/P_c$  ratio was 1.322 (Table XXVI). The Prabakaran equation overestimated the failure load by approximately 22 percent as shown by the average  $P_t/P_c$  ratio of 0.783 (Table XXVII). The Santaputra equation, with an average  $P_t/P_c$  ratio of 1.015 (Table XXVIII), gave good correlation between the failure and the computed load. The range of values for  $P_t$  shows that the bolt patterns did not have a significant impact on the strength of the sections tested.

The failure modes that were observed during the experimental investigation were recorded by taking photographs of the specimens under loading. Photographs of typical the type of bolt patterns used to inter-connect webs of C-sections to form I-sections are shown in Figures 21 through 23. The failure modes that resulted from the IOF loading condition were observed to be a local bearing type of failure directly under the applied concentrated load.

## C. EVALUATION OF RESULTS

1. Statistical Comparison of Results: Table XXIX is used to compare the tested results of this study to the calculated results found by using the AISI equation, the

Table XXIX. STATISTICAL DATA

Specimen Type	AISI Multiple Web Equation		AISI Single Web Equation		Prabakaran Equation		Santaputra Equation	
	Mean $P_t/P_c$	COV	Mean $P_t/P_c$	COV	Mean $P_t/P_c$	COV	Mean $P_t/P_c$	COV
Z	NA	NA	1.078	0.164	0.667	0.125	1.000	0.085
Z-F	NA	NA	1.512	0.140	0.937	0.103	1.409	0.093
I	0.848	0.019	1.239*	0.030	0.743	0.017	0.973	0.007
I-F	0.880	0.030	1.283*	0.038	0.768	0.032	1.010	0.022

\* AISI Single Web Equation was used for I-sections due to the large bolt spacing used to inter-connect the C-sections. This bolt spacing prevented the webs of the C-sections from obtaining proper web interaction, therefore each web acted as a single web.

F = Represents specimens having flanges fastened to supports.

COV = Coefficient of Variation.

NA = Not Applicable.

Prabakaran equation, and the Santaputra equation. This table compares statistical data of tested failure loads to the calculated failure loads of fastened flange specimens and unfastened flange specimens for the Z-section and I-section specimen types. This comparison was done to identify which equation best correlates to the tested data from this investigation. The accuracy of the prediction equations can be assessed by inspecting the ratio of  $P_t/P_c$  for the test specimens.

2. Z-Sections: Tables IX through XX summarize the results of the tests performed on the Z-section specimens subjected to an EOF loading condition with flanges restrained and unrestrained for the AISI web equation, the Prabakaran equation, and the Santaputra equation.

The AISI equation, the Prabakaran equation, and the Santaputra equation yielded the following results for Z-section specimens with flanges unfastened to the supports. The AISI equation yielded  $P_t/P_c$  values that ranged from 0.832 to 1.314 (Tables IX, XII, XV, and XVIII) with a mean value of 1.078 and a coefficient of variation of 0.164 as shown in Table XXIX. The Prabakaran equation, for the same specimens, produced  $P_t/P_c$  ratios of 0.573 to 0.805 (Tables X, XIII, XVI, and XIX) and a mean value of 0.667 and a coefficient of variation of 0.125. The Santaputra equation produced a  $P_t/P_c$  range of 0.842 to 1.131 (Tables XI, XIV, XVII and XX) with a mean value of 1.000 and a coefficient of variation of 0.085. Therefore, for Z-sections with unfastened flanges, the AISI and Santaputra equations produced acceptable web crippling strength predictions.

The AISI equation, the Prabakaran equation, and the Santaputra equation yielded the following results for Z-section specimens with flanges fastened to the supports. The AISI equation yielded  $P_t/P_c$  values that ranged from 1.177 to 1.819 (Tables IX, XII, XV, and XVIII) with a mean value of 1.512 and a coefficient of variation of 0.140 as shown in Table XXIX. The Prabakaran equation, for the same specimens, produced  $P_t/P_c$  ratios of 0.850 to 1.115 (Tables X, XIII, XVI, and XIX) and a mean value of 0.937 and a coefficient of variation of 0.103. The Santaputra equation produced a  $P_t/P_c$  range of 1.118 to 1.572 (Tables XI, XIV, XVII and XX) with a mean value of 1.409 and a coefficient of variation of 0.093. Therefore, for Z-sections with fastened flanges, the



AISI and Santaputra equations largely underestimate web crippling strength and the Prabakaran equation produced an acceptable web crippling strength prediction.

3. I-Sections: Tables XXI through XXVIII summarize the results of the tests performed on the I-section specimens subjected to an IOF loading condition with flanges restrained and unrestrained to supports for the AISI multiple web and single web equations, the Prabakaran equation, and the Santaputra equation.

The AISI multiple web and single web equations, the Prabakaran equation, and the Santaputra equation yielded the following results for I-section specimens with flanges unfastened to the supports. The AISI multiple web equation yielded  $P_t/P_c$  values that ranged from 0.832 to 0.864 (Tables XXI and XXV) with a mean value of 0.848 and a coefficient of variation of 0.019 as shown in Table XXIX. The AISI single web equation yielded  $P_t/P_c$  values that ranged from 1.202 to 1.276 (Tables XXII and XXVI) with a mean value of 1.239 and a coefficient of variation of 0.030. The Prabakaran equation, for the same specimens, produced  $P_t/P_c$  ratios of 0.730 to 0.756 (Tables XXIII and XXVII) and a mean value of 0.743 and a coefficient of variation of 0.017. The Santaputra equation produced a  $P_t/P_c$  range of 0.966 to 0.979 (Tables XXIV and XXVIII) with a mean value of 0.973 and a coefficient of variation of 0.007. Therefore, for I-sections with unfastened flanges, the AISI multiple web equation and the Prabakaran equation yielded unconservative results. The AISI single web equation yielded conservative results, while the Santaputra equation produced good web crippling strength predictions.

The AISI multiple web and single web equations, the Prabakaran equation, and the Santaputra equation yielded the following results for I-section specimens with flanges

fastened to the supports. The AISI multiple web equation yielded  $P_t/P_c$  values that ranged from 0.842 to 0.936 (Tables XXI and XXV) with a mean value of 0.880 and a coefficient of variation of 0.030 as shown in Table XXIX. The AISI single web equation yielded  $P_t/P_c$  values that ranged from 1.216 to 1.381 (Tables XXII and XXVI) with a mean value of 1.283 and a coefficient of variation of 0.038. The Prabakaran equation, for the same specimens, produced  $P_t/P_c$  ratios of 0.733 to 0.819 (Tables XXIII and XXVII) and a mean value of 0.768 and a coefficient of variation of 0.032. The Santaputra equation produced a  $P_t/P_c$  range of 0.978 to 1.061 (Tables XXIV and XXVIII) with a mean value of 1.010 and a coefficient of variation of 0.022. Therefore, for I-sections with fastened flanges, the AISI multiple web equation and the Prabakaran equation yielded unconservative results. The AISI single web equation yielded conservative results, while the Santaputra equation produced good web crippling strength predictions.

#### D. DEVELOPMENT OF FLANGE RESTRAINT FACTOR FOR Z-SECTIONS

The Z-sections tested in this study, which were subjected to EOF loading conditions, showed a significant increase in strength when the restraining effect of the flanges is considered. The restraining effect of fastening the flanges to the supports greatly increases the web crippling capacity of the Z-sections subjected to an EOF loading condition.

Tables IX through XX show the average  $P_t/P_{uf}$  values determined in this study. These average  $P_t/P_{uf}$  values ranged from 1.328 to 1.551. The AISI equation was

developed based on test specimens not having their flanges restrained to the supports. This would indicate that the AISI equation used to calculate the web crippling capacity is underestimating the web crippling strength of the fastened flange specimens. The trend of this behavior can be seen by Figure 24,  $P_f/P_{uf}$  vs.  $h/t$ . The data from this study and test data obtained from similar type Z-sections developed by Bhakta [6] are shown in Figure 25 to show the good correlation between the two study's. Based on a regression analysis of the data of this study, the following flange restraint factor equation was derived:

$$\frac{P_f}{P_{uf}} = 1.16 + \frac{25.72}{h/t} \quad (\text{Eq. 24})$$

Equation 24 applies only to Z-sections subjected to an EOF loading condition having the following limitations as defined by the test program:  $0.059 \leq t \leq 0.083$  in.,  $70 \leq h/t \leq 151$ ,  $3 \leq R/t \leq 4.25$ ,  $31 \leq N/t \leq 45$ ,  $0.25 \leq N/h \leq 0.50$ ,  $56 \leq F_y \leq 74$  ksi.

The correlation between Eq. 24 and the test data can be seen on Figure 24. The existing AISI equation used to calculate the unfastened flange web crippling strength can be modified to obtain the fastened flange web crippling strength by multiplying by Eq. 24. If the Bhakta data is considered (Figure 25), the flange restraint factor can conservatively be taken as 1.30 having the above limits. Either approach will result in a considerable increase in web crippling strength and provide a more accurate representation of the web crippling strength of Z-sections with fastened flanges subjected to only an EOF loading condition.

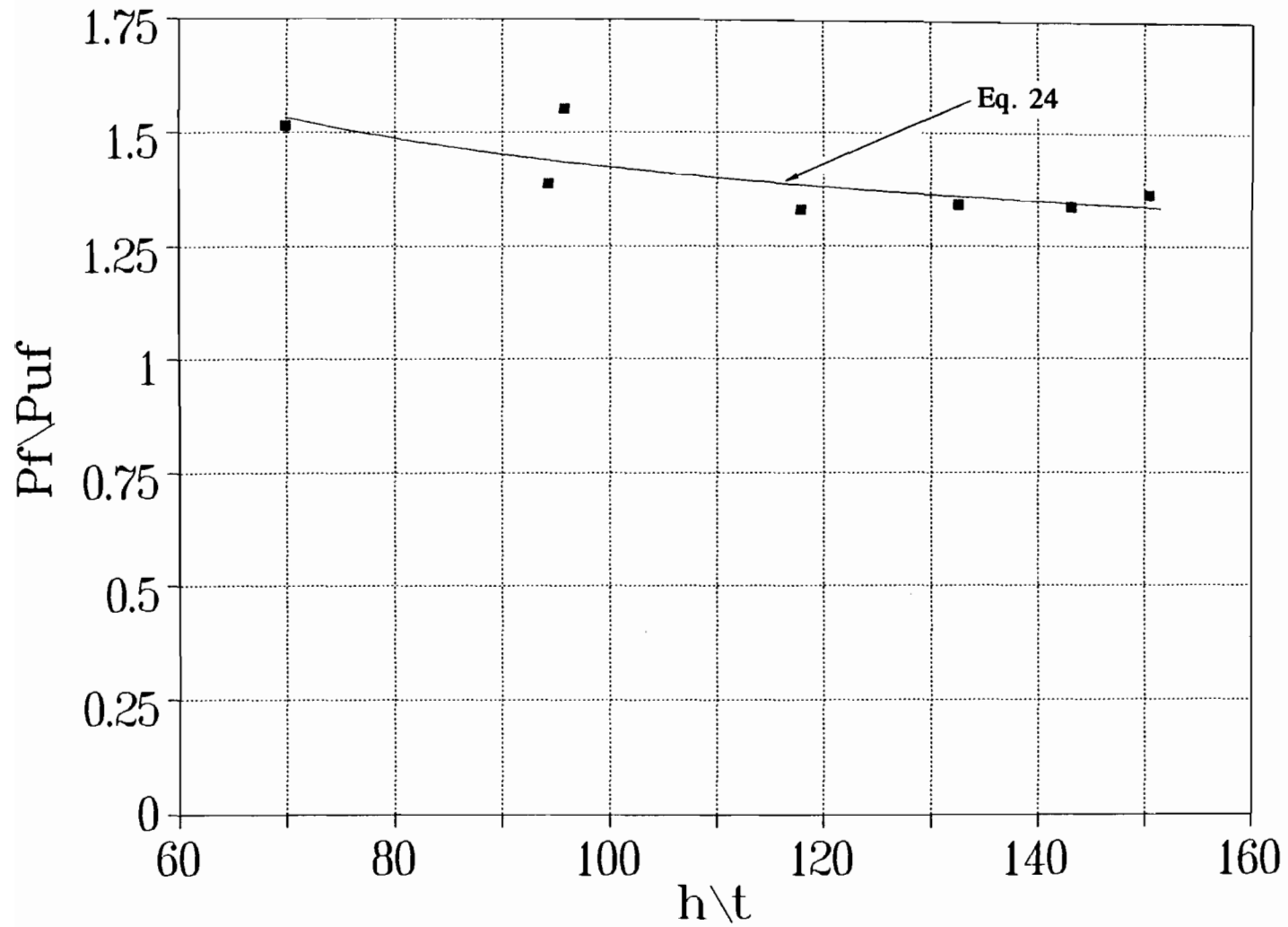


Figure 24. Graph of  $P_f/P_{uf}$  vs.  $h/t$  for Fastened Flange Z-Sections Showing the Suggested Modification Curve

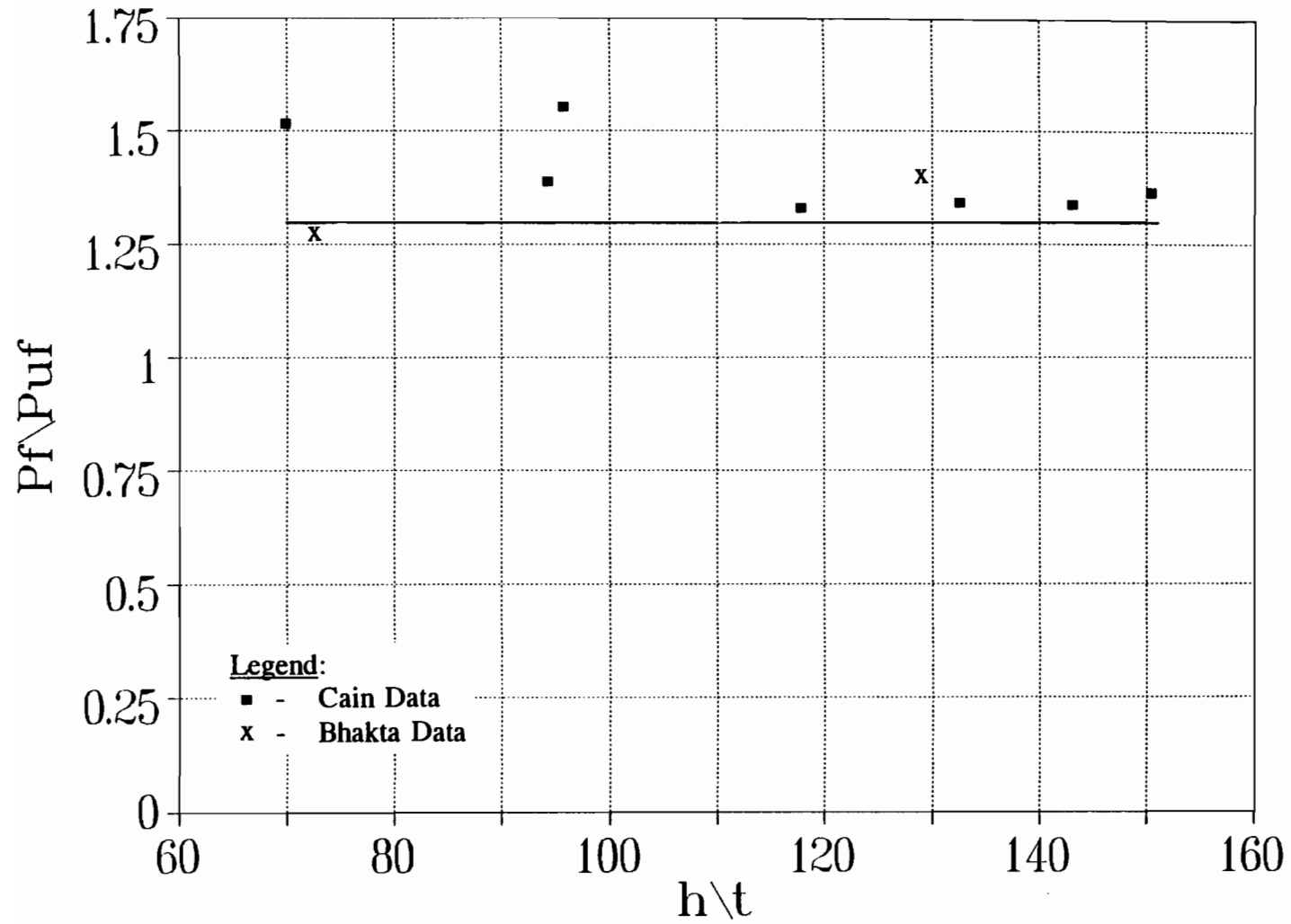


Figure 25. Graph of  $P_f/P_{uf}$  vs.  $h/t$  for Fastened Flange Z-Sections Including Bhakta Data Points

## V. PROPOSED DESIGN RECOMMENDATIONS

Based on the limited test results from 28 Z-section specimens and 14 I-section specimens obtained in this study, the following design recommendations are made:

(1) For Z-sections with unrestrained flanges subjected to an EOF loading condition, the existing AISI Specification [3] strength equation is a good conservative predictor of the web crippling strength.

(2) For Z-sections with restrained flanges subjected to an EOF loading condition, proposed design modifications in Section IV.D are suggested for the existing AISI Specification [3] to conservatively predict the web crippling strength. The unmodified AISI Specification equation and the Santaputra, Parks and Yu equation [8] underestimated the tested results, while the Prabakaran and Schuster equation [7] slightly overestimated the tested load.

(3) For the I-section with unrestrained and restrained flanges subjected to an IOF loading condition, the existing AISI Specification single web equation [3] is a conservative predictor of the web crippling strength. The AISI Specification multiple web equation and the Prabakaran and Schuster equation [7] overestimated the tested failure loads. The Santaputra, Parks and Yu equation [8] provided an acceptable estimate of the tested results.

## V. CONCLUSIONS

The objective of this experimental investigation was to explore the conservative and unconservative aspects of the present design provisions for web crippling of Z-sections subjected to an end one-flange loading (EOF) condition and I-sections subjected to an interior one-flange loading (IOF) condition. This phase of the investigation focused only on the EOF loading condition of Z-sections to further study the web crippling capacity of the Z-section members with their flanges fastened to the support. This study also focused only on the IOF loading condition of back-to-back C-sections to form I-sections to study the effect of fastened flange web crippling strength due to the bolt configuration used to inter-connect the sections together. Based on the tests performed and results obtained the following conclusions were formed:

The Z-sections tested in this study which were subjected to EOF loading conditions showed a significant increase in load carrying capability when the restraining effect of the flanges was considered.

The I-sections tested in this study which were subjected to IOF loading conditions yielded approximately the same failure loads regardless of flange attachment or type of bolt pattern used to inter-connect the specimens.

## BIBLIOGRAPHY

1. Walker, A. C., "Design and Analysis of Cold Formed Sections," International Textbook Company Limited, London, U.K., 1975.
2. Yu, W. W., Cold Formed Steel Design. Second Edition, John Wiley and Sons, Inc., New York, 1991.
3. American Iron and Steel Institute, "Cold-Formed Steel Design Manual: Specification for the Design of Cold-Formed Steel Structural Members," August 19, 1986, with December 11, 1989 Addendum.
4. Winter, G., and R. H. J. Pian, "Crushing Strength of Thin Steel Webs," Cornell Bulletin No. 35, Part 1, Engineering Experiment Station, Cornell University, April 1946.
5. Hetrakul, N., and W. W. Yu, "Structural Behavior of Beam Webs Subjected to Web Crippling and a Combination of Web Crippling and Bending," Final Report, Civil Engineering Study 78-4, University of Missouri-Rolla, Rolla, Missouri, June 1978.
6. Bhakta, B. H., R. A. LaBoube, and W. W. Yu, "The Effect of Flange Restraint on Web Crippling Strength," Final Report, Civil Engineering Study 92-1, University of Missouri-Rolla, Rolla, Missouri, March 1992.
7. Prabakaran, K., and R. M. Schuster, "Web Crippling of Cold Formed Steel Sections," Project Report, Department of Civil Engineering, University of Waterloo, Waterloo, Canada, April 1993.
8. Santaputra, C. M., B. Parks, and W. W. Yu, "Web-Crippling Strength of Cold-Formed Steel Beams," Journal of the Structural Division, ASCE, Vol. 115, No. 10, October 1989.
9. Sommerfeld, A., Zeitschrift für Mathematik und Physik, vol. 54, 1906.
10. Timoshenko, S. P., Zeitschrift für Mathematik und Physik, vol. 58, 1910.
11. Leggett, D. M. A., "The Effect of Two Isolated Forces on Elastic Stability of Flat Rectangular Plate," Proceedings, Cambridge Philosophical Society, vol. 33, 1937.
12. Hopkins, H. G., "Elastic Stability of Infinite Strips," Proceedings, Cambridge Philosophical Society, vol. 45, 1969.



13. Yamaki, H. G., "Buckling of a Rectangular Plate under Locally Distributed Forces Applied on the Two Opposite Edges," 1st, 2nd, and 4th reports, The Institute of High-Speed Mechanics, Tohoku University, Japan, 1953 and 1954.
14. Zetlin, L., "Elastic Instability of Flat Plates Subjected to Partial Edge Loadings," Journal of the Structural Division, ASCE Proceedings, vol. 81, September 1955.
15. White, R. N., and W. S. Cottingham, "Stability of Plates under Partial Edge Loadings," Journal of the Engineering Mechanics Division, ASCE Proceedings, vol. 88, October 1962.
16. Khan, M. Z., and A. C. Walker, "Buckling of Plates Subjected to Localized Edge Loading," The Structural Engineer, vol. 50, June 1972.
17. Khan, M. Z., K. C. Johns, and B. Hayman, "Buckling of Plates with Partially Loaded Edges," Journal of the Structural Division, ASCE Proceedings, vol. 103, March 1977.
18. Timoshenko, S. P., and G. M. Gere, Theory of Elastic Stability, Second Edition, McGraw-Hill Book Company, Inc., New York, 1961.
19. Bakker, M., T. Peköz, and J. Stark, "A Model for the Behavior of Thin-Walled Flexural Members Under Concentrated Loads," Proceedings of the Tenth International Specialty Conference on Cold-Formed Steel Structures, University of Missouri-Rolla, October 23-24, 1990.
20. Santaputra, C., and W. W. Yu, "Web Crippling of High Strength Cold-Formed Steel Beams," Final Report, Civil Engineering Study 86-1, University of Missouri-Rolla, Rolla, Missouri, August 1986.
21. Bagchi, D. K., and K. C. Rokey, "A Note on the Buckling of a Plate Girder Web Due to Partial Edge Loadings," Final Report, International Association for Bridge and Structural Engineering, September 1968.
22. Rokey, K. C., and D. K. Bagchi, "Buckling of Plate Girder Webs under Partial Edge Loadings," International Journal of Mechanical Science, vol. 12, Pergamon Press.
23. Rokey, K. C., M. A. El-gaaly, and D. K. Bagchi, "Failure of Thin Walled Members under Patch Loadings," Journal of the Structural Division, ASCE Proceedings, vol. 98, December 1972.
24. Graves Smith, T. R., and S. Sridharan, "A Finite Strip Method for the Buckling of Plate Structures under Arbitrary Loading," International Journal of Mechanical Science, vol. 20, May 1978.

25. Gierlinski, J. T., and T. R. Graves Smith, "The Geometric Nonlinear Analysis of Thin-Walled Structures by Finite Strips," Thin-Walled Structures, Elsevier Applied Science Publishers Ltd., Great Britain, 1984.
26. Lee, H. P., P. J. Harris, and C. T. Hsu, "A Nonlinear Finite Element Computer Program for Thin-Walled Members," Thin-Walled Structures, Elsevier Applied Science Publishers, Ltd., Great Britain, 1984.
27. American Iron and Steel Institute, "Cold-Formed Steel Design Manual: Specification for the Design of Cold-Formed Steel Structural Members," 1968.
28. American Iron and Steel Institute, "Cold-Formed Steel Design Manual: Specification for the Design of Cold-Formed Steel Structural Members," 1980.
29. American Iron and Steel Institute, "Automotive Steel Design Manual," 1986.
30. Langan, J. E., R. A. LaBoube, and W. W. Yu, "Structural Behavior of Perforated Web Elements of Cold-Formed Steel Flexural Members Subjected to Web Crippling and a Combination of Web Crippling and Bending," Final Report, Civil Engineering Study 94-3, University of Missouri-Rolla, Rolla, Missouri, 1994.
31. American Society for Testing and Materials, ASTM, A370-77, 1977.